EAST WEST UNIVERSITY

Department of EEE

***Section*:** 01
***Course Code*:** EEE308
***Course Name*:** Electronic Properties of Materials
Semester: Summer 2023

Simulation of Thin-Film Solar Cells based on (CCZTSe) Using (SCAPS-1D) Program

Course Instructor:

Shovon Talukder, Lecturer, EEE, EWU

Rohit Bhowmick

ID: 2020-1-80-006

ABSTRACT

This study presents the outcomes of a computer-simulated investigation on a thin-film solar cell utilizing a p-type CCZTSe absorber layer and an n-type CdS buffer layer within a structure of (WS_2+CCZTSe+CdS+ITO). The simulation software used was SCAPS-1D. The thickness of the absorber layer varied within the range of 0.25 to 3 µm, and a single type of defect was introduced to the absorber layer to enhance the cell's realism. The results demonstrated that altering the CCZTSe layer thickness led to an enhancement in the conversion efficiency (η), from 23.94% to 25.06%, peaking at 25.06% with a thickness of 0.75µm. Moreover, the short-circuit current density (J_{SC}) increased from 44.21315 to 51.694313 mA/cm². Introducing defects densities (N_{def}) ranging from 10^{14} to 10^{17} cm⁻³ leads to an efficiency drop from 27.77% to 13.01%. The FF decreased from 83.19% to around 63.36%, J_{SC} decreased from 51.432857 to 41.400155 mA/cm², and V_{OC} decreased from about 0.649 V to approximately 0.4531 V. However, increasing the acceptor concentration (N_A) in the CCZTSe absorption layer within the range of 10^{14} to 10^{20} cm⁻³ leads to efficiency (η) improvement from roughly 19.61% to about 33.24%. FF increased from 71.34% to 84.95%, and V_{OC} increased from 0.5351 V to 0.7681 V, while J_{SC} remained relatively consistent. Altering the donor density (N_D) in the CdS buffer layer did not induce any noticeable changes.

OBJECTIVES

The objective of the project seems to be focused on studying and analyzing the performance of thin-film solar cells based on a specific material, which in this case is Copper-Cadmium Zinc Tin Selenide (CCZTSe), using a simulation program called SCAPS-1D. Thin-film solar cells are characterized by their use of thin semiconductor layers to absorb and convert sunlight into electricity. The solar cells being studied in this project are based on the Copper-Cadmium Zinc Tin Selenide (CCZTSe) material. This indicates that the project involves researching and modeling the behavior of solar cells that use CCZTSe as the absorber material. CCZTSe is a type of semiconductor material that has shown promise for photovoltaic applications due to its potential for efficient light absorption and energy conversion. The aim to achieve the high efficiency photovoltaic cell by manipulating the absorber layer thickness and defect density, exploring their influence on the overall performance of the solar cell.

INTRODUCTION

The growing global demand for energy has placed energy production at the forefront of the world's challenges. Solar energy (SE) has emerged as a viable alternative to fossil fuels, offering environmentally friendly solutions. Among the various methods of harnessing solar energy, solar cells play a crucial role by directly converting sunlight into electrical energy. This study proposes the use of a Thin-Film (CCZTSe) solar cell to achieve both high efficiency and cost-effectiveness. By alloying different ratios of $Cu_2ZnSnSe_4$(CZTS) and $Cu_2CdSnSe_4$ (CCTS), the energy gap can be tuned within the range of 1.05 to 1.5 eV. However, the presence of impurities can potentially lower the conversion efficiency of the solar cell. Expanding the absorption of light into the infrared spectrum is a desirable goal.

Employed the simulation software (SCAPS-1D) to investigate a photovoltaic cell composed of a (ZNO) window layer, a (CCZTSe) absorption layer, and a (CdS) buffer layer. The research demonstrated that the CCZTSe layer holds promise for infrared radiation detection. Building upon this, the current researchers intend to utilize the same software, SCAPS-1D, to create a high-efficiency photovoltaic cell.

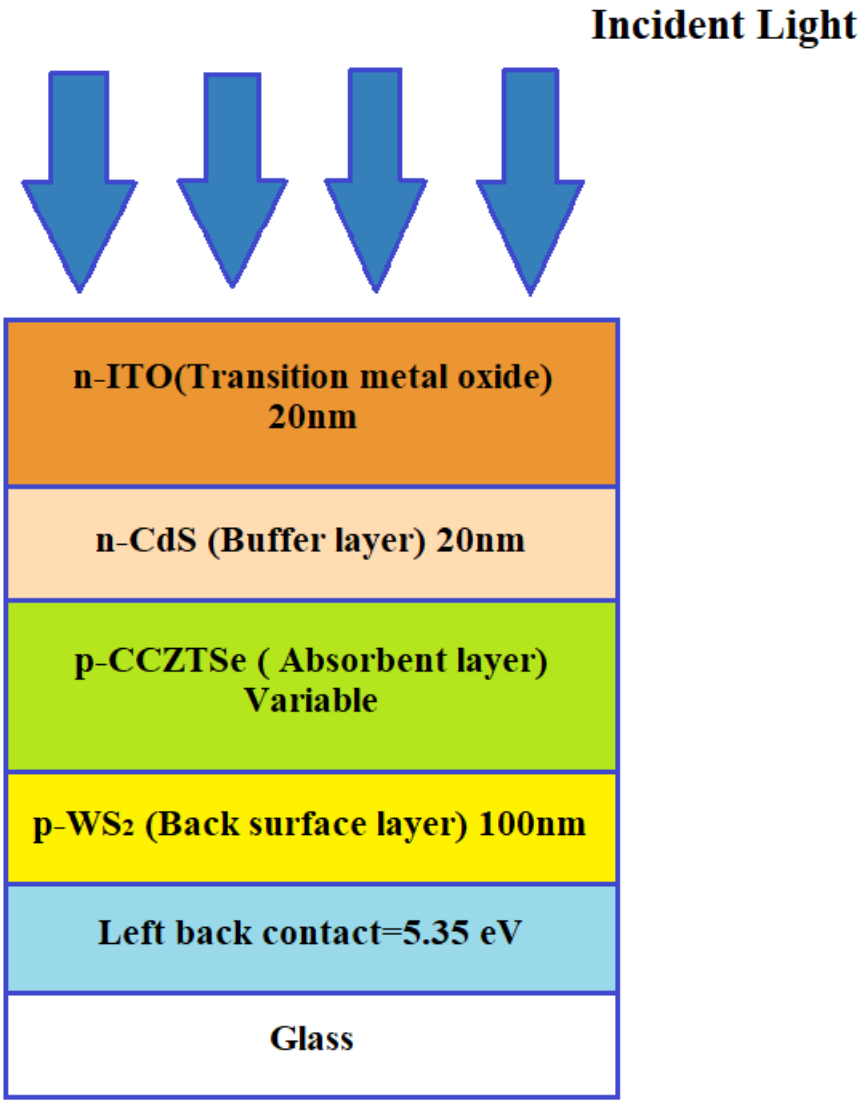

Figure 01: Solar cell installation construction WS_2+CCZTSe+CdS+ITO

INSTRUCTION TO SIMULATE SCAPS-1D

SCAPS (a Solar Cell Capacitance Simulator) is a one-dimensional solar cell simulation program. SCAPS-1D is a computer simulation tool developed by the Electronics and Information Systems (ELIS) department at Ghent University. This one-dimensional software, offered as open-source, is designed to facilitate various solar research endeavors. s. I-V, C-V, C-f, and QE characteristics can be obtained from the simulation easily.

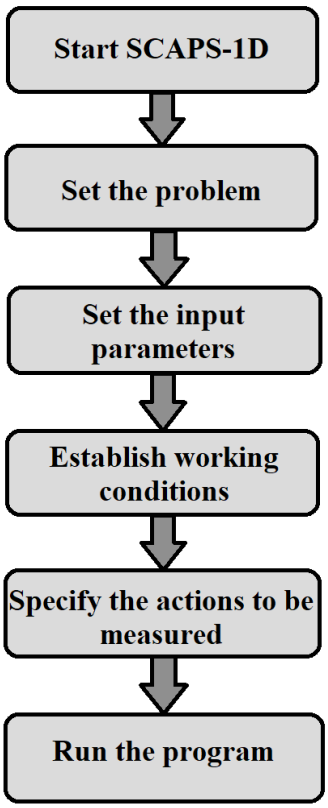

Figure 02: Steps to build and simulate a solar cell in SCAPS -1D

NUMERICAL MODELING & MATERIAL PARAMETERS

Computer simulations have proven to be effective in analyzing photovoltaic devices, enabling the assessment of the optical, electrical, and mechanical properties. By providing valuable insights into intricate photovoltaic systems, these simulations offer a feasible approach to enhance device performance. This, in turn, could lead to a reduction in manufacturing expenses and researcher workload. Offering practical recommendations for optimizing production parameters to boost device efficiency can further contribute to this endeavor.

The solar cell depicted in Figure 1 was replicated and simulated using the SCAPS-1D software. The experimental conditions were set at a temperature of 300^0 K. To calculate essential parameters such as open-circuit voltage (V_{OC}), short-circuit current density (J_{SC}), fill factor (FF), efficiency (η), and quantum efficiency (QE), a series of equations numbered from equation (*i*) to equation (*v*) were applied in the analysis,

The simulation program sets the global default light spectrum at 1.5AM with a light intensity of 1000 (W/cm^2).

The Open-Circuit-Voltage (V_{OC}) when the load resistance is infinite is given by Equation (*i*). It is obvious that V_{OC} depends on I_L(light-generated current or photovoltaic-current) and the saturation-current I_0.

$$V_{OC} = \frac{nKT}{q} \ln\left(\frac{I_L}{I_O} + 1\right) \text{ at I=0} \ldots\ldots\ldots\ldots\ldots (i)$$

The short-circuit-current density (J_{SC}) is defined as the greatest output current-density when the cell is short circuited.

$$J_{SC}(V) = J_O(e^{qV/nK_BT} - 1) \ldots\ldots\ldots\ldots\ldots (ii)$$

Where (J_O) is the saturation-current-density. There are several factors that affect the short circuit current, the intensity of lamination, cell optical properties and p-n junction thickness.

The Fill-Factor (FF) of the cell is given by:

$$FF = \frac{V_{mp} \cdot J_{mp}}{J_{OC} \cdot V_{OC}} \ldots\ldots\ldots\ldots\ldots (iii)$$

The FF typically falls within the (0.70-0.85)% range.

The conversion-efficiency (η) is given by:

$$\eta = \frac{P_{mp}}{P_{in}} = \frac{V_{OC} \cdot J_{SC} \cdot FF}{P_{in}} \ldots\ldots\ldots\ldots\ldots (iv)$$

The efficiency of conversion (η) is obtained by dividing the electrical power output by the optical power input.

The quantum-efficiency (QE) is given by:

$$QE = \frac{hcR_\lambda}{q\lambda}$$

$\frac{hc}{q} = 1.24$ is a constant value, hence

$$QE = 1.24\left(\frac{R_\lambda}{\lambda}\right) \ldots\ldots\ldots\ldots\ldots (v)$$

R_λ is the spectral-response in units (A/W), λ is the wavelength (nm). Quantum efficiency (QE) can be defined as the quantity of electron-hole pairs generated per photon absorbed by the absorbing layer. This attribute holds significant importance in photovoltaic uses. The simulation program sets the global default light spectrum at 1.5AM with a light intensity of 1000 (W/m^2). The depicted cell structure (refer to Figure 1) comprises several layers. It initiates with a transparent layer composed of transition-metal oxide (ITO), followed by an n-type buffer semiconductor layer made of cadmium-sulfide (CdS). This CdS layer possesses a substantial energy gap and a high refractive index, facilitating the creation

of the necessary n-p junction with the subsequent p-type CCZTSe absorbing layer. Positioned after this is a p-type layer composed of tungsten-disulfide (WS_2) material. This WS_2 layer plays a pivotal role in channeling electrons back to enhance the cell's performance. The n-p junction forms between the CdS layer and the absorbing layer, enabling efficient electron movement.

PARAMETER

Table 01: The main parameters of the solar cell (CCZTSe)

Parameters	Symbol (Unit)	CCZTSe	WS2	CdS	ITO
Thickness	d (µm)	Variable	0.1	0.02	0.02
Band Gap	Eg (eV)	0.9	1.29	2.4	3.6
Electron affinity	χ (eV)	4.4	4.05	4.2	4.1
Dielectric permittivity	rϵ/ϵ	10	13.6	10	10
CB effective density of states	$N_a(cm^{-3})$	2.2×10^{18}	2.2×10^{18}	2.2×10^{18}	2×10^{18}
VB effective density of states	$N_V(cm^{-3})$	1.8×10^{19}	1.8×10^{19}	1.8×10^{19}	1.8×10^{19}
Electron thermal velocity	V_n(cm/s)	1×10^{7}	1×10^{7}	1×10^{7}	1×10^{7}
Hole thermal velocity	V_P(cm/s)	1×10^{7}	1×10^{7}	1×10^{7}	1×10^{7}
Electron mobility	μ_n(cm^2/v.s)	60	100	100	50
Hole mobility	μ_p(cm^2/v.s)	20	100	25	75
donor density	N_D(cm^{-3})	0	0	Variable	1×10^{18}
acceptor density	N_A(cm^{-3})	Variable	1×10^{18}	0	0
Characteristic energy in a Gauss defect distribution	W_G(eV)	0.1	0.1	0.1	0.1
Defect Density	N_{def}(cm^{-3})	Variable	2×10^{12}	5×10^{17}	1×10^{15}
Electron capture cross section	σ_e(cm^2)	10^{-15}	10^{-12}	10^{-15}	10^{-12}
Hole capture cross section	σ_h(cm^2)	10^{-15}	10^{-15}	10^{-15}	10^{-15}

Table 2: ***Interface Gaussian Defect States of the solar cell (CCZTSe)***

Parameters	Symbol (Unit)	CCZTSe/CdS
Gaussian defect density	N_t(cm^{-3})	1×10^{15}
Electron capture cross section	σ_e(cm^2)	1×10^{-16}
Electron capture cross section	σ_h(cm^2)	1×10^{-15}

RESULTS AND DISCUSSION:

- ***Effect of changing the thickness of the absorbent layer***

Table 01 provides an overview of the key parameters of the cell (refer to ***Figure 01***). In order to investigate the impact of the absorber layer's thickness on performance, variations were made in the thickness of the absorbing layer (p-CCZTSe), ranging from 0.25 to 3 µm. Throughout this analysis, the concentration of defect density (N_{def}) remained initially consistent at 10^{14} cm^{-3}. The thickness of the buffer layer (BSL), the window layer, and the buffer layer itself were maintained at a constant value of 0.1 µm, 0.02 µm, and 0.02 µm, respectively. In the model, we made the assumption of a consistent presence of interface defects at the CCZTSe/CdS junction, with a density of 10^{15} cm^{-3}. ***Table 02*** presents data concerning the concentration of interface defects and their corresponding capture cross-sections. As the thickness of the absorber layer is augmented, the absorption of photons also rises, consequently resulting in improvements in the cell's characteristics. Defects within the range of 10^{13} to 10^{17} cm^{-3} were introduced into the absorption layer to enhance the alignment of the simulation model with real-world conditions. This incorporation of defects aimed to explore their impact on the properties of the cell. A single type of defect was introduced to maintain model simplicity. The purpose of introducing defects was to potentially enhance electrical conductivity or regulate cell performance. However, it's worth noting that an excessive concentration of defects could potentially lead to a decrease in the conversion efficiency of the cell. In ***Figure 05***, there is a noticeable rise in the short-circuit current density (J_{SC}) observed, increasing from 44.21315 mA/cm² at a thickness of 0.25 µm to 51.694313 mA/cm² at a thickness of 3 µm. As the thickness increases, there is a modest decline in the open circuit voltage (V_{OC}), shifting from (0.6345V) at a thickness of (0.25µm) to (0.5681V) at a thickness of (3µm).

In ***Figure 04***, the quantum efficiency (QE) is displayed in relation to photon wavelength, with the thickness of the absorber layer as the varying parameter. Notably, ***Figure 04*** reveals that the quantum efficiency (QE) reached its highest point as the absorber layer thickness was increased. This outcome indicates that incident photons of varying wavelengths were absorbed at distinct depths within the photovoltaic cell.

In ***Figure 05***, the relationship between the thickness of the p-CCZTSe absorption layer and two key parameters, namely (J_{SC}) and (V_{OC}), is depicted. As the thickness of the (p-CCZTSe) layer increases, the (J_{SC}) of the cell demonstrates an upward trend. This phenomenon can be attributed to the fact that a thicker absorber layer has the capability to absorb a greater number of longer-wavelength photons, resulting in the creation of more electron-hole pairs. The figure illustrates a slight decline in the (V_{OC}) values as the thickness increases, transitioning from 0.6345V to 0.5681V.

In ***Figure 06,*** the enhancement in conversion efficiency (η) becomes apparent as the thickness of the absorber layer (p-CCZTSe) increases. The efficiency rises from approximately 22.75% to 25.06% within the thickness range spanning from 0.25 µm to 0.75 µm and decreases from 25.04% to 23.94 within the thickness range spanning from 1µm to 3µm. This increase in efficiency can be ascribed to the creation of a voltage barrier between the back reflection layer and the absorbing layer. The presence of the back reflection layer

functions to redirect electrons, averting their accumulation and consequently mitigating the recombination process. This effect leads to an overall increase in cell efficiency.

Moreover, the fill factor (FF) experiences a minor increase from 81.58% at a thickness of 0.25 µm to a peak of 81.88% at 1 µm, subsequently showing a slight decline to 79.74% when the thickness reaches 3.0 µm, as depicted in ***Figure 06***.

Cell properties when changing the thickness in the p-CCZTSe absorbent layer, the concentration of defects density (N_{def}) & acceptor density of CCZTSe and the donor density of CdS initially is kept constant at ($10^{14}cm^{-3}$), ($10^{17}cm^{-3}$) & (10^{18} cm^{-3}) respectively.

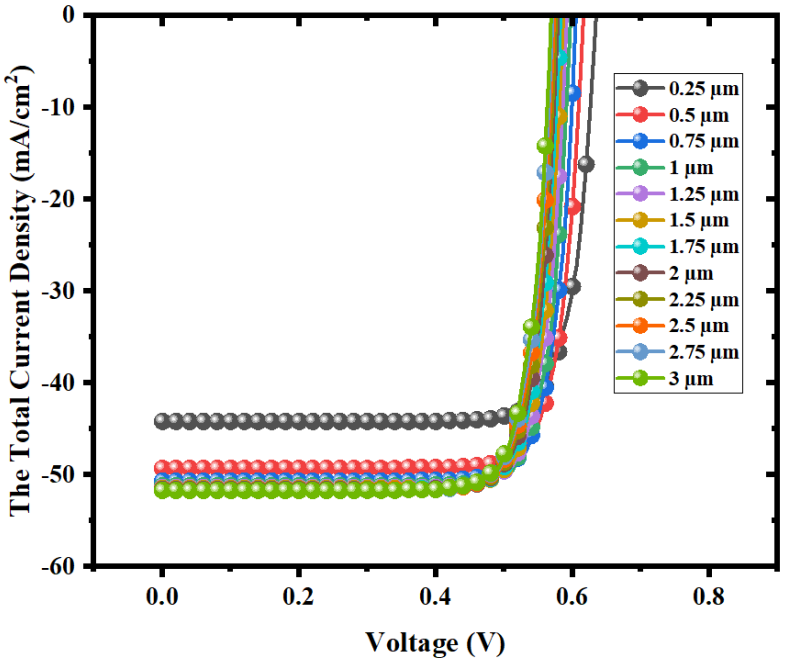

[Data Table: https://shorturl.at/LRYZ3]

Figure 03: Effect of the Thickness of the p-CCZTSe absorption layer on the (I-V) curve

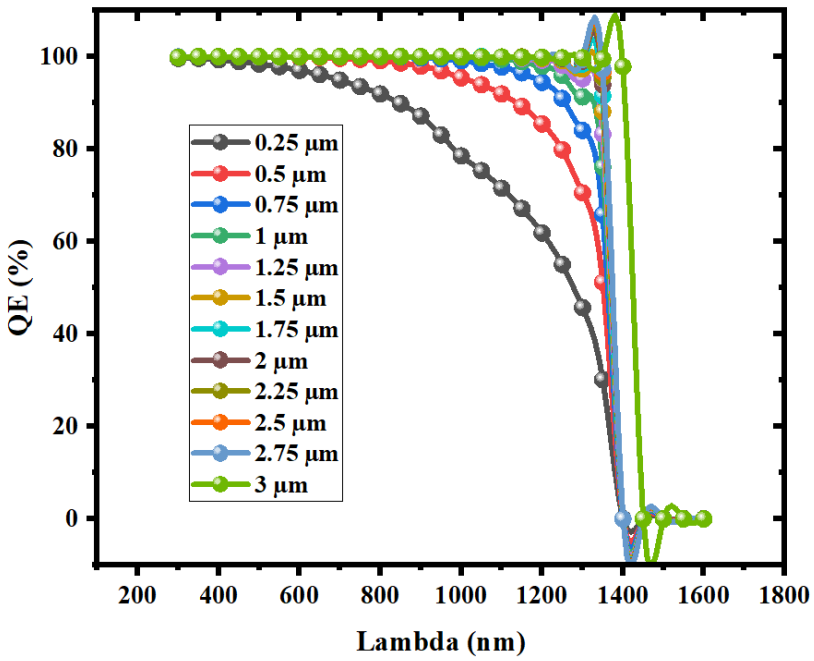

[Data Table: https://shorturl.at/uUW37]

Figure 04: Effect of Thickness on Quantum-efficiency (QE) Curve

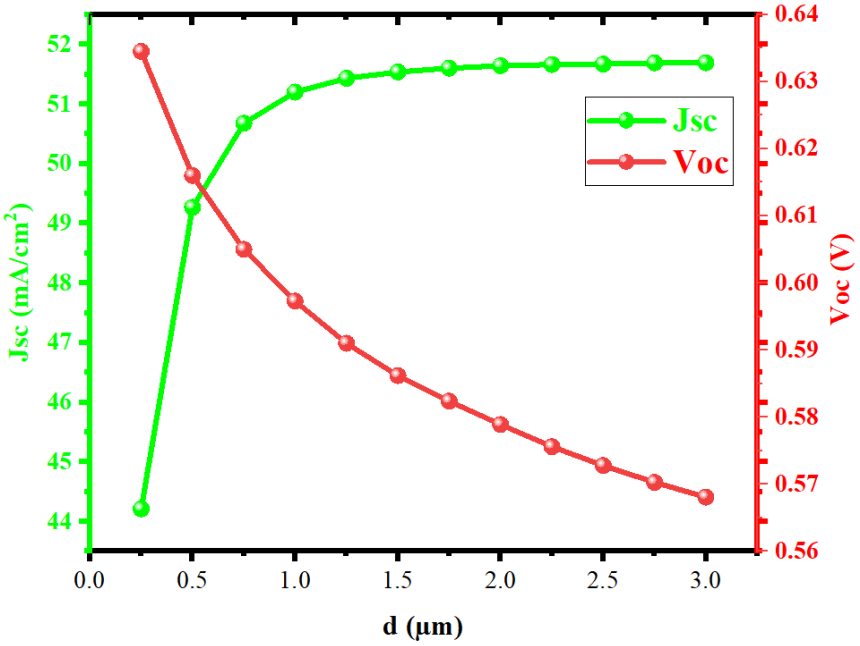

[Data Table: https://rb.gy/xcif2]

Figure 05: Effect of the Thickness of the p-CCZTSe absorption layer on the open circuit voltage (V_{OC}) and current density (J_{SC})

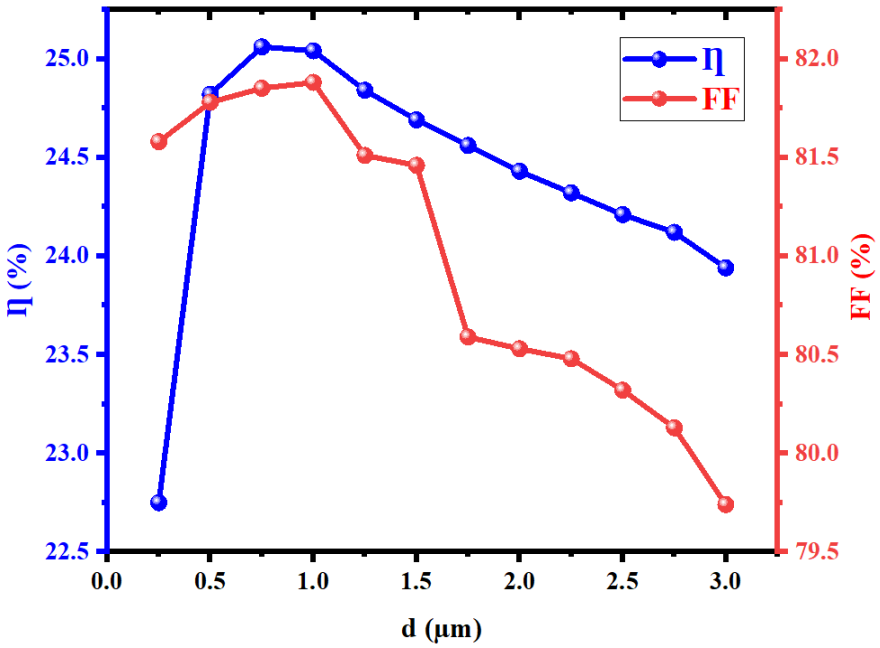

[Data Table: https://rb.gy/xcif2]

Figure 06: Effect of the Thickness of the p-CCZTSe absorption layer on the efficiency value (Η) and fill factor (FF)

- ***Effect of Acceptor Concentration***

The density of acceptors (N_A) within the absorption layer was varied within the range of 10^{14} to 10^{20} cm^{-3}, while keeping the thickness constant at 1.25 µm. In ***Figure 07***, the impact on open-circuit voltage (V_{OC}) and short-circuit current density (J_{SC}) is illustrated. Additionally, ***Figure 08*** portrays the influence on efficiency (η) and Fill Factor (FF). The open-circuit voltage (V_{OC}) experiences an increase from 0.5351V when the acceptor concentration (N_A) is set at 10^{14} cm^{-3}, to 0.7687V as the acceptor concentration is elevated to 10^{20} cm^{-3}. However, the alteration in the short-circuit current density (J_{SC}) is generally minimal. Within the same range of N_A variation mentioned earlier, the efficiency of the cell showed improvement, rising from 19.61% to 33.24%. Likewise, the fill factor (FF) experienced an increase, ranging from 71.31% to 84.95%. The primary underlying factor for this phenomenon is the elevation in acceptor concentration. This increase leads to a subsequent rise in the device's saturation current. Consequently, the open-circuit voltage (V_{OC}) also experiences an increase. This adjustment allows the absorption of photons with longer wavelengths and lower energy levels to penetrate deeper into the (CCZTSe) absorption layer. Therefore, the efficiency of conversion is greatly influenced by alterations in the acceptor concentration. As evident from ***Figure 08***, both the efficiency (η) and fill factor (FF) demonstrate enhancement.

Cell properties when changing the acceptor density (N_A) in the p-CCZTSe absorbent layer, the thickness and defect density of CCZTSe, donor density of CdS is kept at (1.25 µm), ($10^{14}cm^{-3}$), ($10^{18}cm^{-3}$) respectively.

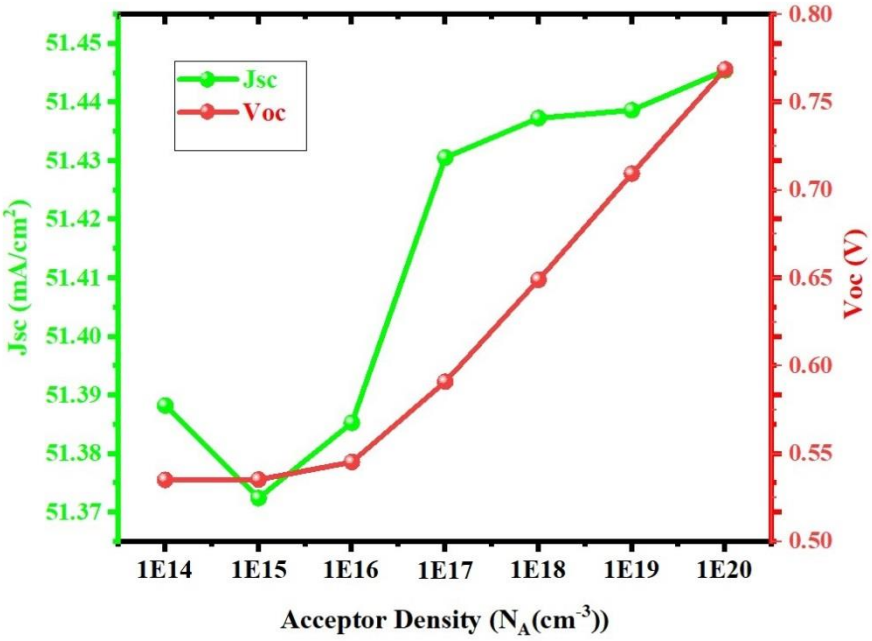

[Data Table: https://t.ly/KCdpL]

Figure 07: Effect of Acceptor Concentration in the absorption layer on the current density (J_{SC}) and open circuit voltage (V_{OC})

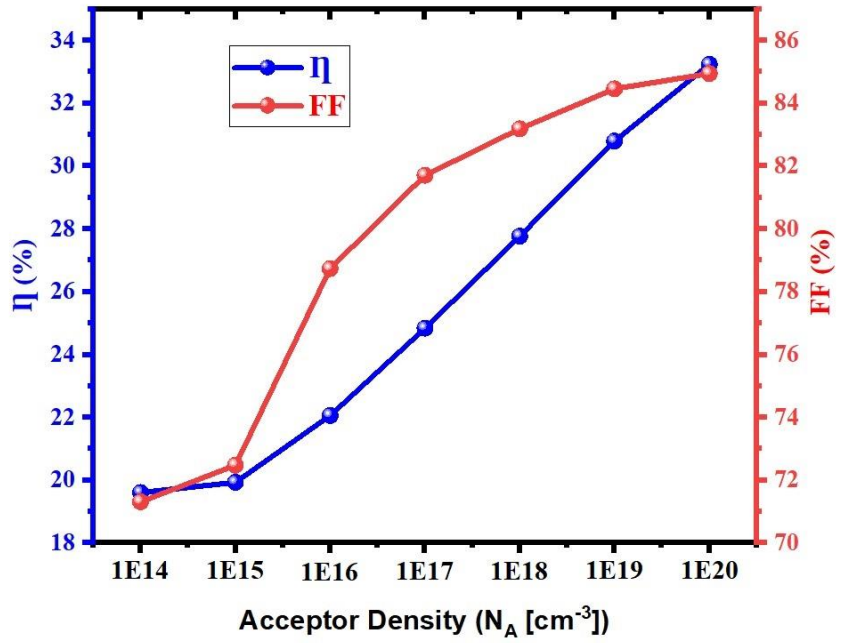

[Data Table: https://t.ly/KCdpL]

Figure 08: Effect of Acceptor Concentration in the absorption layer on cell efficiency (Ƞ) and filling factor (FF)

- ***Effect of Donor Concentration***

The density of donors (N_D) within the n-CdS buffer layer was varied within the range of 10^{14} to 10^{20} cm^{-3}, while keeping the thickness and acceptor concentration of the absorbent layer constant at 1.25 µm & 10^{18} cm^{-3}. As indicated in ***figure 09***, the alterations in (V_{OC}) and (J_{SC}) are relatively minimal. Similarly, the change in the conversion-efficiency (Ƞ) is negligible as shown in ***Figure 10***. The filling factor (FF) remains almost constant at about 83.45% up to 10^{17} cm^{-3}, as shown in ***Figure 10.***

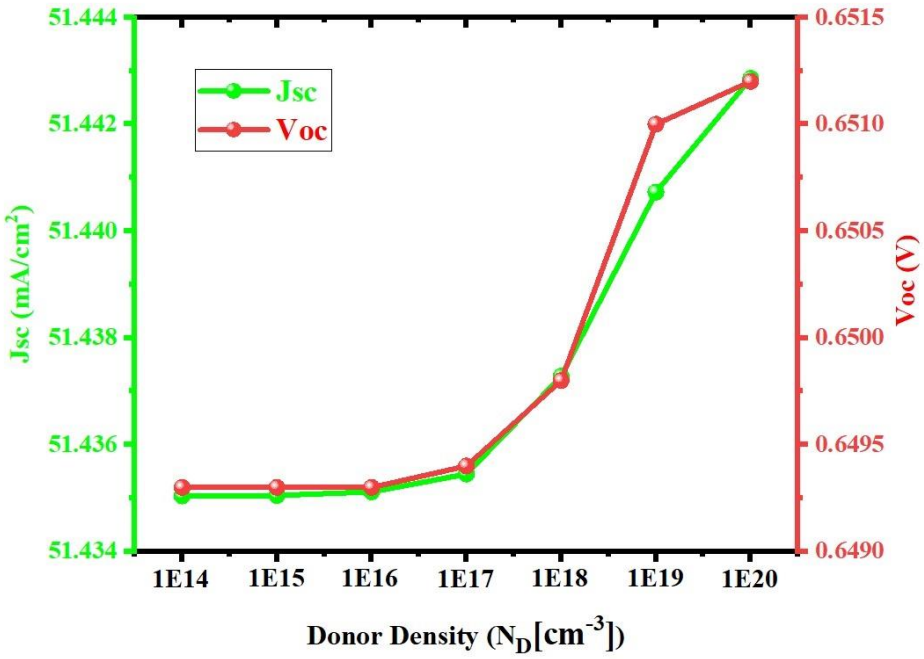

[Data Table: https://t.ly/6H7I]

Figure 09: Effect of donor concentration (N_D) in the n-CdS layer on V_{OC} and J_{SC}

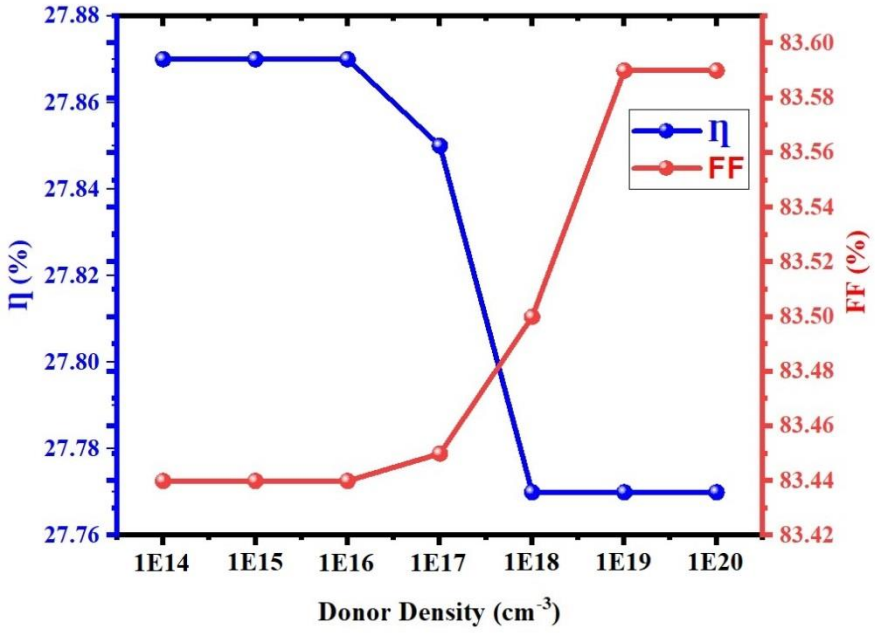

[Data Table: https://t.ly/6H7I_]

Figure 10: Effect of the donor concentration (ND) in the n-CdS layer on the cell efficiency (Ƞ) and the filling factor (FF)

- **Effect of defects density in the absorbent layer**

The influence of defects on the p-CCZTSe absorption layer was examined across a concentration spectrum spanning from 10^{14} to 10^{17} cm^{-3}. This investigation maintained a constant absorber layer thickness of 1.25 µm and an acceptor concentration of 10^{18} cm^{-3}. The donor-concentration in the CdS- layer was constant at 10^{20} cm^{-3}.

Figure 11 displays the current-voltage (I-V) curves corresponding to different defect densities. As the density of defects within the absorbent layer increases, both the open-circuit voltage (V_{OC}) and the short-circuit current (J_{SC}) exhibit a decrease. This trend is evident in ***Figure 12***, which further illustrates the relationship between defect density and these key parameters. The decrease in values for open-circuit voltage (V_{OC}) and short-circuit current (J_{SC}) could potentially be attributed to the heightened presence of trapping centers for minority carriers. This heightened presence subsequently results in an increase in the rate of recombination, leading to a reduction in the open circuit voltage. This behavior is a consequence of the recombination process occurring within the material and at the semiconductor surfaces.

The efficiency value decreases from (27.77%) at a defect-density (10^{14} cm^{-3}) to (13.01%) at ($10^{17}cm^{-3}$) which is displayed in ***Figure 13***. The value of the fill factor (FF) is reduced from (83.19%) at a defect-density of (10^{13} cm^{-3}) to (69.36%) at (10^{17} cm^{-3}), which is also displayed in the ***figure 13***.

The fill factor (FF) undergoes a decrease, transitioning from 83.19% when the defect density is at 10^{14} cm^{-3} to 69.36% at a defect density of 10^{17} cm^{-3}. This alteration is also visually depicted in ***figure 13***. The decline in both open-circuit voltage and fill factor results in a decrease in efficiency, as explained in Equation (*vi*). This decrease can be attributed to the presence of recombination current within the depletion region and an elevated recombination process at the interface. In terms of quantum efficiency (QE), the value stands at 27.77% with a defect density of 10^{14} cm^{-3}. However, this value diminishes to 13.01% when the defect density is raised to 10^{17} cm^{-3}, as illustrated in ***figure 14***.

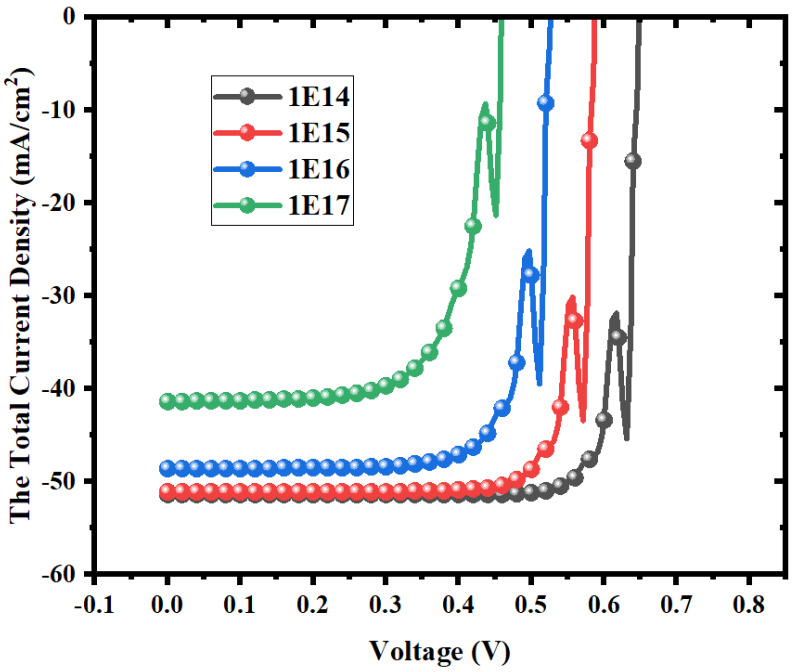

[Data Table: https://t.ly/BYTIN]

Figure 11: Effect of defect density in p-CCZTSe absorption layer on the I-V curve

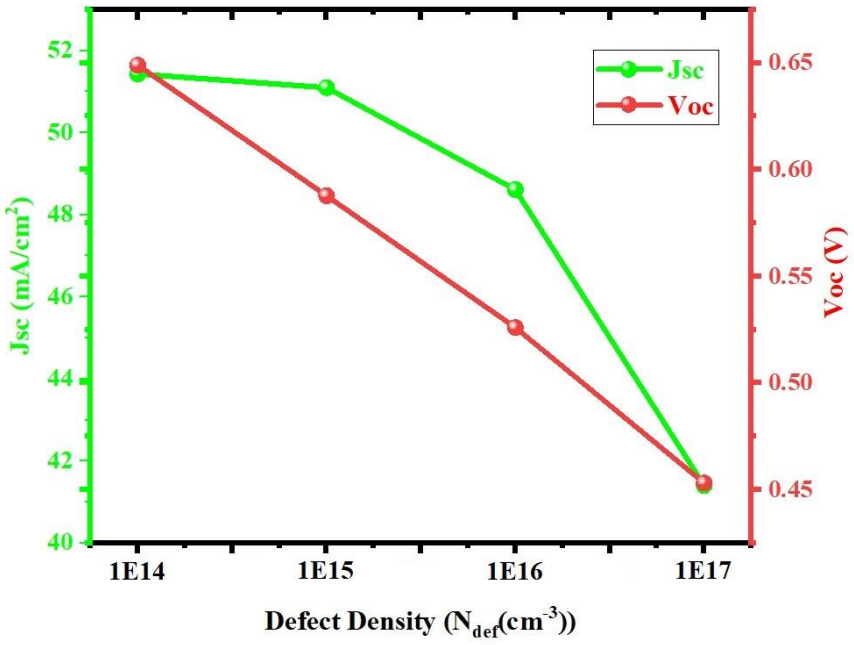

[Data Table: https://t.ly/fqulu]

Figure 12: Effect of the defect density in the p-CCZTSe absorption layer on V_{OC} and J_{SC}

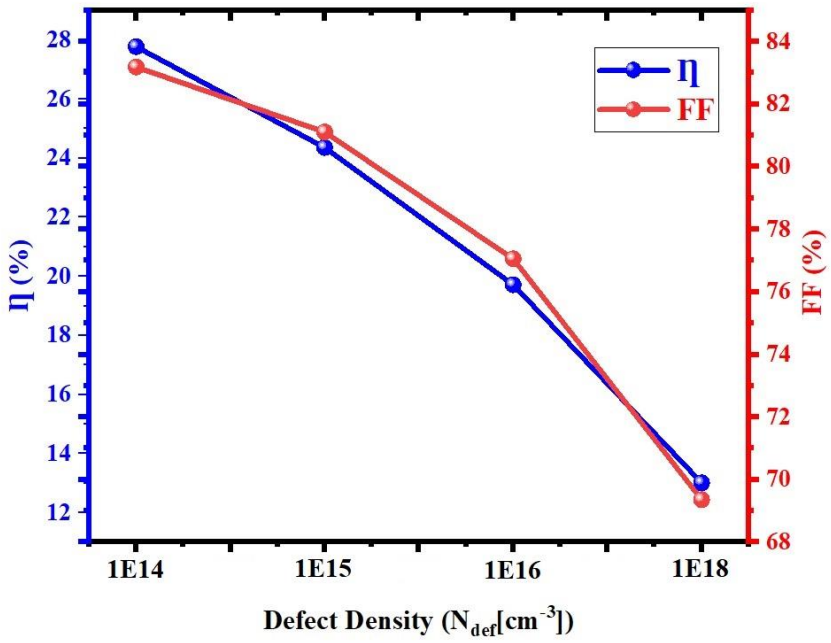

[Data Table: https://t.ly/fqulu]

Figure 13: Effect of the defect density of the p-CCZTSe adsorption layer on the efficiency value (Η) and fill factor (FF)

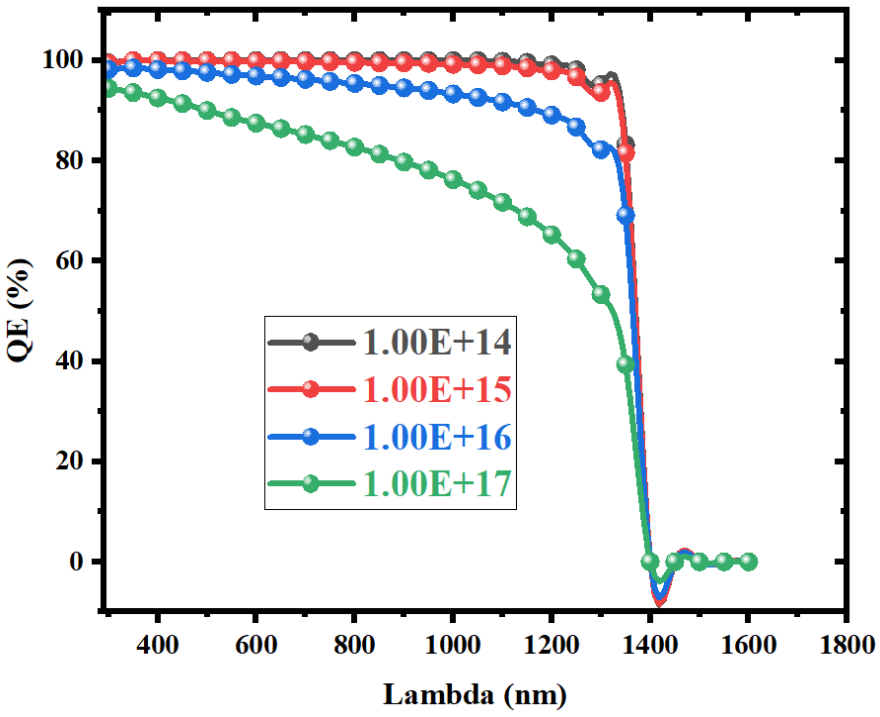

[Data Table: https://t.ly/5YJod]

Figure 14: Effect of defect density (N_{def}) on the Quantum efficiency (QE)

❖ ***EFFECT OF TEMPERATURE***

Working temperature plays a major role in the performance of a device. Generally, the testing temperature of a solar cell device is at 300^{O} K, but at the installed conditions, the working temperature is more than 300^{O}K. In this case, the absorber is considered with the defect density of 10^{14} cm^{-3}. The operating temperature varied from 295^{O}K – 325^{O}K and then the changes in the characteristics are observed and given in ***figure 15 & 16***.

Cell properties when changing the temperature, the thickness, concentration of defects density (N_{def}) & acceptor density of CCZTSe and the donor density of CdS initially is kept constant at (1.25 μm), (10^{14} cm^{-3}), ($10^{17}cm^{-3}$) & (10^{18} cm^{-3}) respectively.

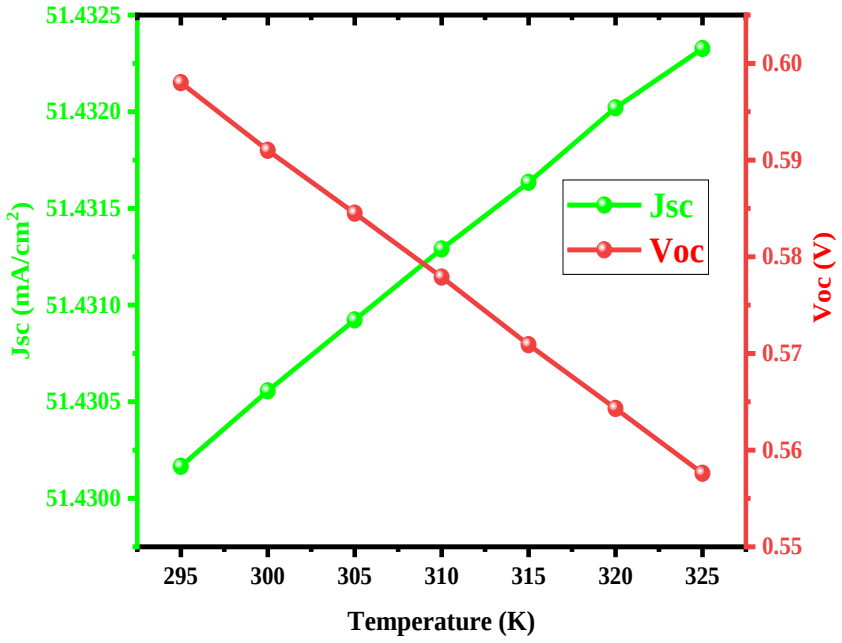

[Data Table: https://tinyurl.com/5cje42xy]

Figure 15: Effect of the Temperature in the p-CCZTSe based solar cell on V_{OC} and J_{SC}

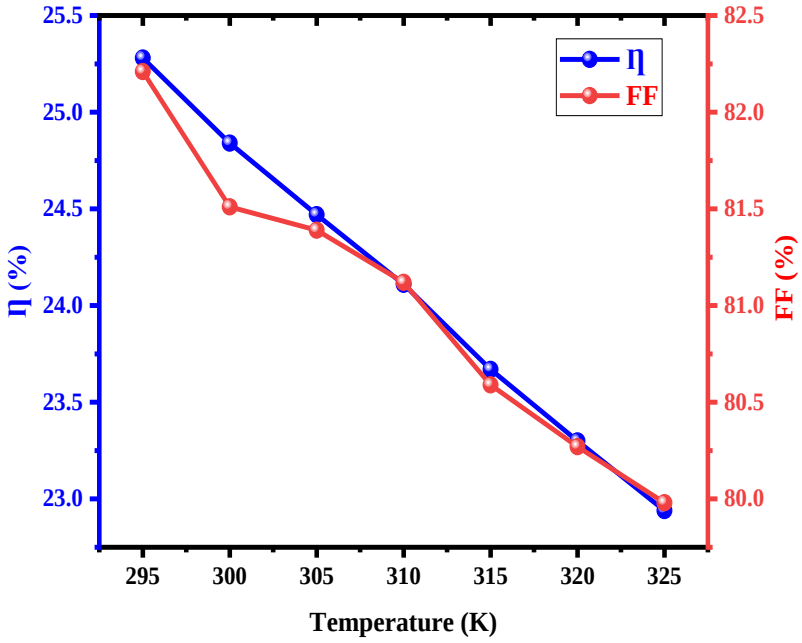

[Data Table: https://tinyurl.com/5cje42xy]

Figure 16: Effect of the Temperature in the p-CCZTSe based solar cell on the efficiency value (Ƞ) and fill factor (FF)

PHYSICS

In this project we find two physics involved after looking at the simulation results. The first is defect and the other is temperature.

First we discuss the defect. Efficiency is an important factor for solar cells. Elevated defect density within the absorber layer of solar cells has been identified as a leading cause for reduced cell performance. As defect density rises, the quantum efficiency of the cells diminishes. Research indicates that the ideal defect density for the absorption layer stands at 10^{14} cm^{-3}. Beyond this threshold, the effectiveness of the solar cell experiences a decline. If we look at ***figure 13***, we see that the efficiency (Ƞ) decreases as we increase the number of defects (N_{def}) in the absorption layer.

Second comes temperature. The performance of a device is significantly influenced by the temperature at which it operates. While solar cell devices are typically tested at a temperature of 300^{O}K, it's important to note that their actual working temperature after installation can exceed this value. In such instances, when studying a solar cell's behavior, it's essential to consider the absorber's defect density, which is around 10^{14} cm^{-3}. The experiment involves varying the operating temperature within the range of 295^{O} K to 325^{O} K and observing the resultant changes in the device's characteristics. These observed variations in characteristics are illustrated in ***figures 15*** and ***16***. If we look at ***figure 16***, we see that the efficiency (Ƞ) decreases as we increase the temperatures (T) of this solar system.

Elevated temperatures have an adverse impact on the efficiency of solar panels. These panels are initially evaluated under standard testing conditions at 25°C (about 298.15°K). However, in real-world scenarios, the

efficiency of photovoltaic modules can decrease by around (10-25) % due to the heat generated by their installation location.

We can also calculate the efficiency theoretically using equation (*iv*)

$$\eta = \frac{P_{mp}}{P_{in}} = \frac{V_{OC} \cdot J_{SC} \cdot FF}{P_{in}}$$

Here, V_{OC} is open circuit voltage, J_{SC} is short circuit current density, FF is fill factor the efficiency of conversion (η) is obtained by dividing the electrical power output by the optical power input.

PARAMETER FOR $CH_3NH_3Pb(I_{1-x}Cl_x)_3$ BASED PEROVSKITE SOLAR CELL

Table 03: The main parameters of the solar cell $[CH_3NH_3Pb(I_{1-x}Cl_x)_3]$

Parameters	Symbol (Unit)	FTO	TiO_2(ETL)	$CH_3NH_3Pb(I_{1-x}Cl_x)_3$	Cu_2O
Thickness	d (nm)	400	40	450	250
Band Gap	Eg (eV)	3.5	3.2	1.55	2.17
Electron affinity	χ (eV)	4	3.9	3.93	3.2
Dielectric permittivity	rϵ/ϵ	9	9	6.5	7.11
CB effective density of states	$N_a(cm^{-3})$	2.02×10^{18}	1×10^{21}	2.2×10^{17}	2.02×10^{17}
VB effective density of states	$N_V(cm^{-3})$	1.8×10^{19}	2×10^{20}	1.8×10^{19}	1.1×10^{19}
Electron thermal velocity	V_n(cm/s)	1×10^{7}	1×10^{7}	1×10^{7}	1×10^{7}
Hole thermal velocity	V_P(cm/s)	1×10^{7}	1×10^{7}	1×10^{7}	1×10^{7}
Electron mobility	μ_n(cm^2/v.s)	20	20	0.2	200
Hole mobility	μ_p(cm^2/v.s)	10	10	0.2	80
donor density	N_D(cm^{-3})	2×10^{19}	1×10^{19}	-	-
acceptor density	N_A(cm^{-3})	-	1×10^{0}	-	1×10^{18}
Defect Density	N_{def}(cm^{-3})	1×10^{15}	1×10^{15}	1×10^{14}	1×10^{14}
Electron capture cross section	σ_e(cm^2)	10^{-15}	10^{-15}	10^{-15}	10^{-15}
Hole capture cross section	σ_h(cm^2)	10^{-15}	10^{-15}	10^{-15}	10^{-15}

Table 04: ***Interface Gaussian Defect States of the solar cell (CCZTSe)***

Parameters	Cu2O(HTL) / CH3NH3P	$CH_3NH_3Pb(I_{1-x}Cl_x)_3$
Defect Types	Neutral	Neutral
Capture cross section of electrons (cm^2)	10^{-19}	10^{-19}
Capture cross section of holes (cm^2)	10^{-19}	10^{-19}
Energetic distribution	0.6	0.6
Total defect density (cm^{-2})	10^{10}	10^{10}

COMPARISON

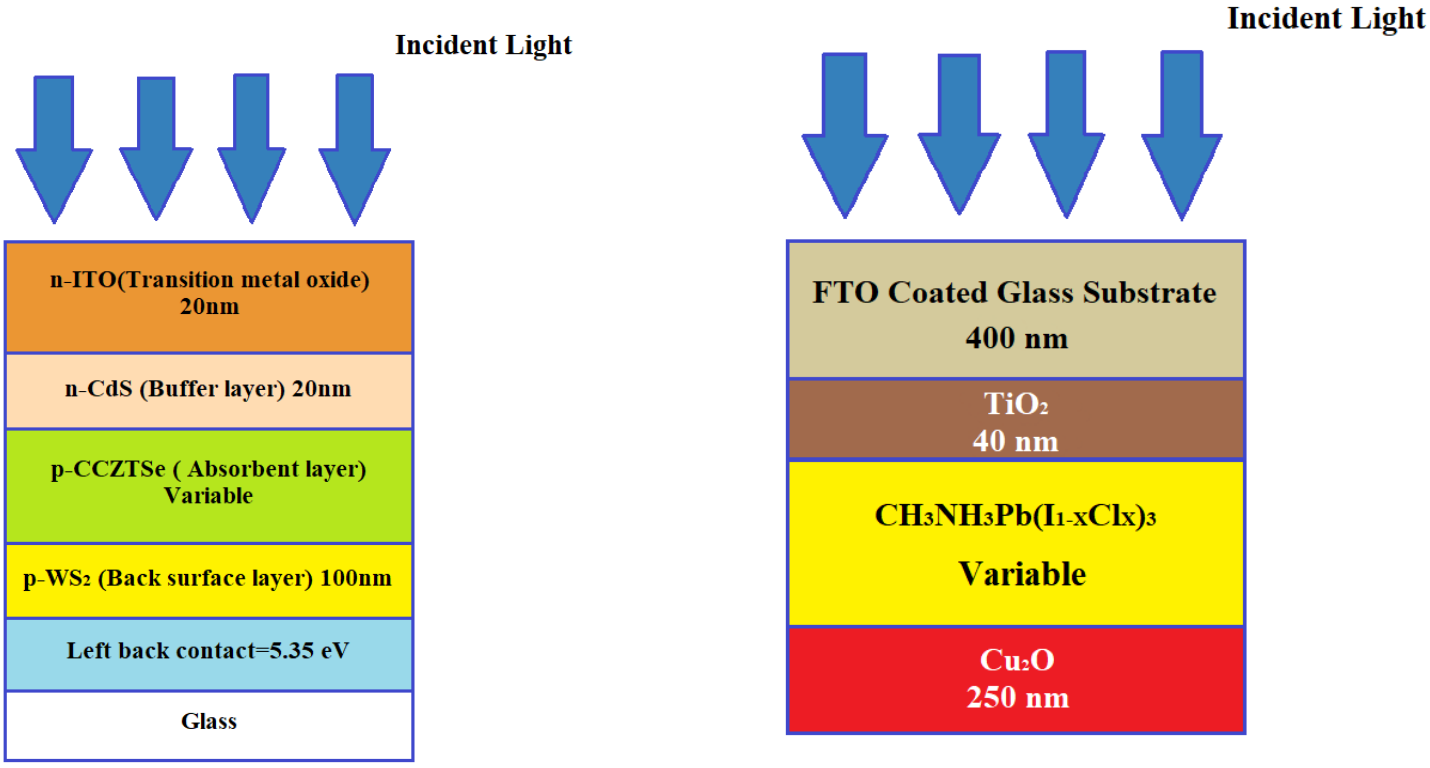

(a) (b)

Figure 17: **(a)** Solar cell installation construction WS2+CCZTSe+CdS+ITO; **(b)** Solar cell installation construction Cu_2O+$CH_3NH_3Pb(I_{1-x}Cl_x)_3$+$TiO_2$+FTO

In ***Figure 14(a)***, Cadmium sulfide (CdS) is a material commonly used in thin-film solar cells, particularly in the context of certain photovoltaic technologies like cadmium telluride (CdTe) solar cells. While CdS-based solar cells can offer certain advantages such as low cost and high efficiency, there are also environmental concerns associated with the use of cadmium, a heavy metal, in these devices. Cadmium is classified as a hazardous substance due to its toxic nature and potential to bioaccumulate in ecosystems. During the manufacturing, use, and disposal of CdS-based solar cells, there is a risk of cadmium being released into the

environment. Cadmium is known to be harmful to human health, especially if ingested or inhaled. Prolonged exposure to cadmium can lead to various health issues, including lung and prostate cancers, kidney damage, and bone diseases. Workers in solar cell manufacturing and recycling facilities may be particularly at risk if proper safety measures are not in place.

❖ ***Effect of changing the thickness of the absorbent layer***

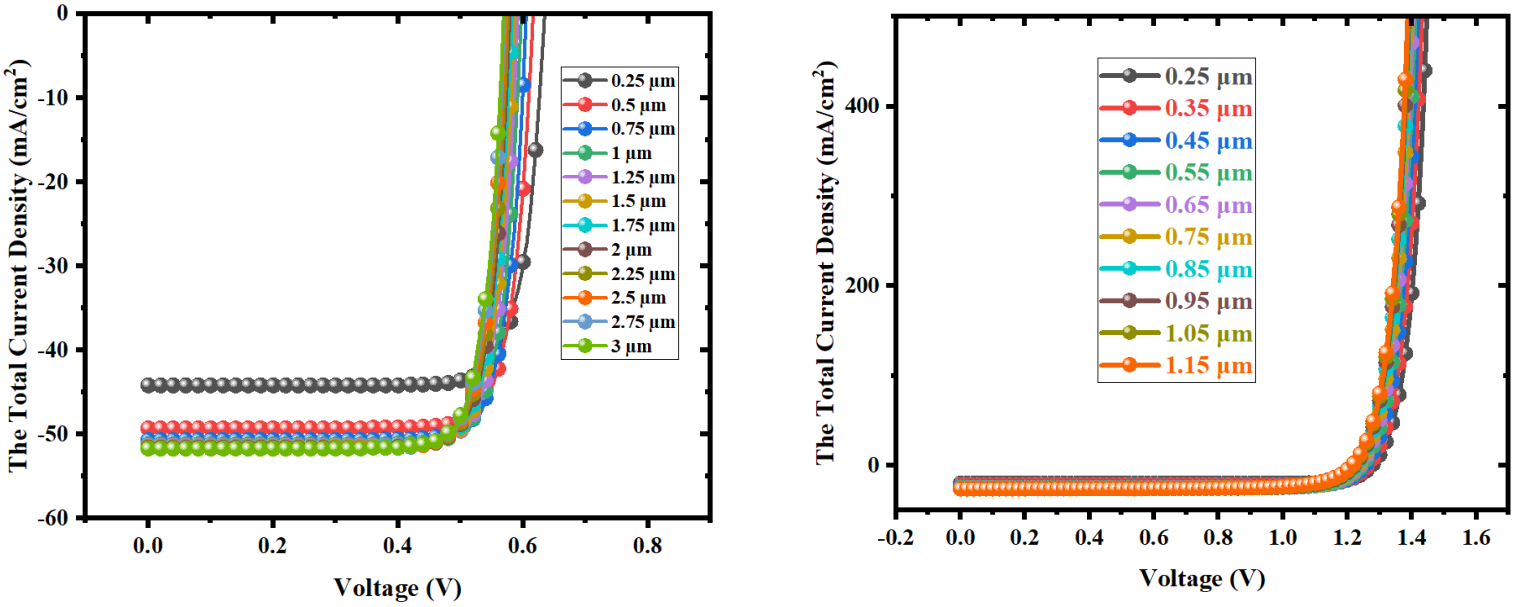

(a) **(b)**

(a)*[Data Table: https://shorturl.at/LRYZ3]*

(b)*[Data Table: https://tinyurl.com/bdetd7t2]*

Figure 18: **(a)** Effect of the Thickness of the p-CCZTSe absorption layer on the (I-V) curve; **(b)** Effect of the Thickness of the $CH_3NH_3Pb(I_{1-x}Cl_x)_3$ absorption layer on the (I-V) curve

In ***figure 18:*(a)** we can see that as thickness increases, V_{OC} decreases (0.6345V-0.5681V) and J_{SC} also increases continuously (44.21315 mA/cm^2-51.694313mA/cm^2). On the other hand, Ƞ also increases to 1 µm after that it starts to decrease again continuously and in the same field of FF it increases up to 1 µm and then decreases again.

In ***figure 18:*(b)** we can see that as thickness increases, V_{OC} decreases (1.2757V-1.2129V) and J_{SC} also increases continuously (19.726473 mA/cm^2-25.695386 mA/cm^2). On the other hand, Ƞ also increases to 0.65 µm after that it starts to decrease again continuously and FF it increases up to 0.55 µm and then decreases again.

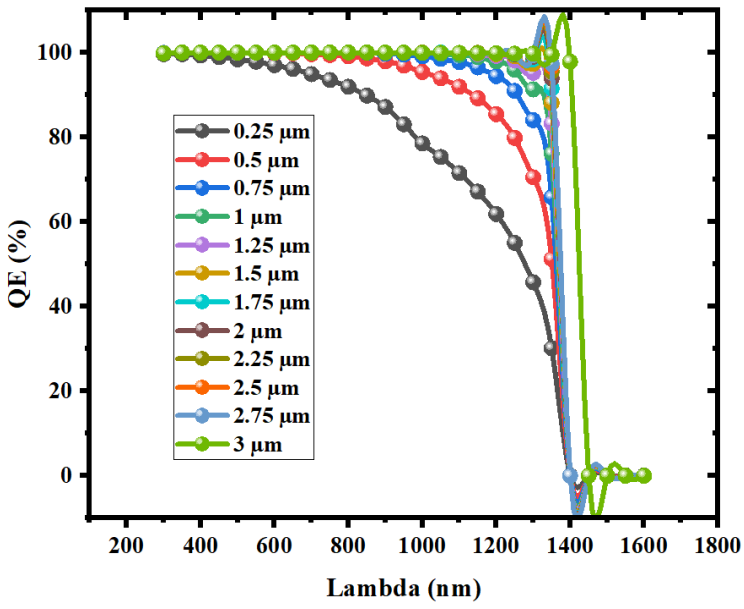

(a)

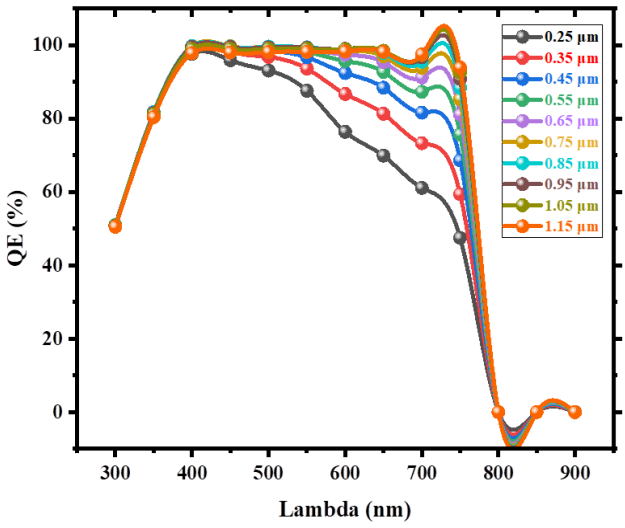

(b)

(a)*[Data Table: https://shorturl.at/uUW37]*

(b)*[Data Table: https://tinyurl.com/4pcc8mpd]*

Figure 19: **(a)** Effect of Thickness on Quantum-efficiency (QE) Curve of CCZTSe layer; **(b)** Effect of Thickness on Quantum-efficiency (QE) Curve of $CH_3NH_3Pb(I_{1-x}Cl_x)_3$ layer

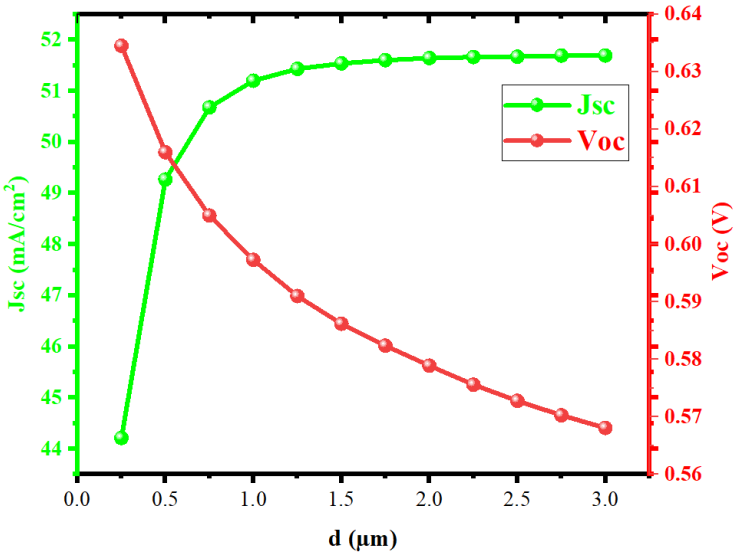

(a)

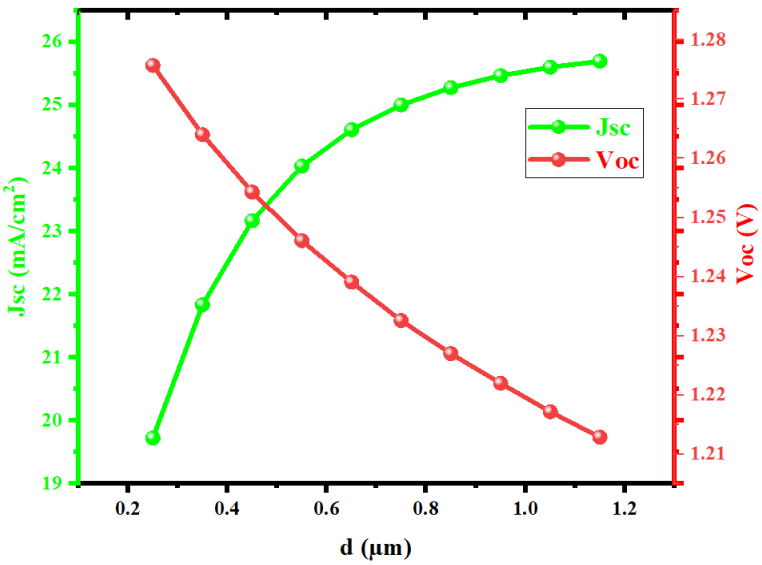

(b)

(a)*[Data Table: https://rb.gy/xcif2]*

(b)*[Data Table: https://tinyurl.com/mm4fsddh]*

Figure 20: **(a)** Effect of the Thickness of the p-CCZTSe absorption layer on the open circuit voltage (V_{OC}) and current density (J_{SC}); **(b)** Effect of the Thickness of the $CH_3NH_3Pb(I_{1-x}Cl_x)_3$ absorption layer on the open circuit voltage (V_{OC}) and current density (J_{SC})

In *figure 20*: (a) we can see that as thickness increases from 0.25 µm to 3 µm, V_{OC} decreases (0.6345V - 0.5681V) and J_{SC} also increases continuously (44.21315 mA/cm^2 - 51.694313mA/cm^2).

In ***figure 20:*(b)** we can see that as thickness increases from 0.25 µm to 1.15 µm, V_{OC} decreases (1.2757V-1.2129V) and J_{SC} also increases continuously (19.726473 mA/cm^2-25.695386 mA/cm^2).

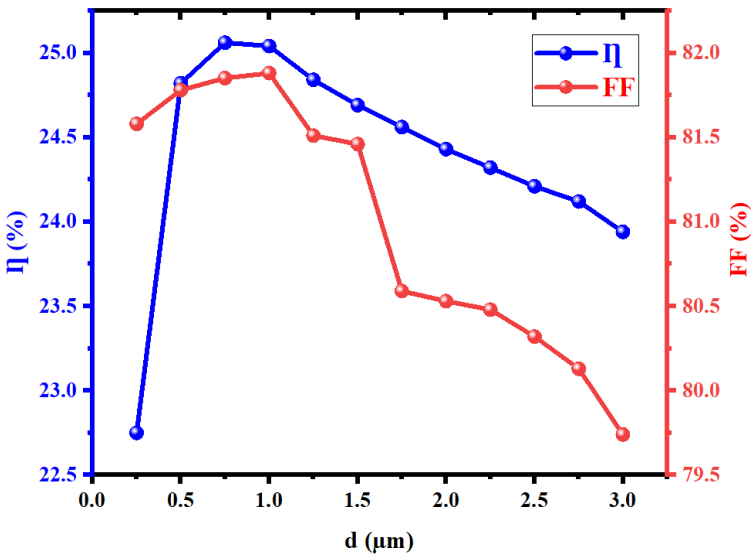

(a)

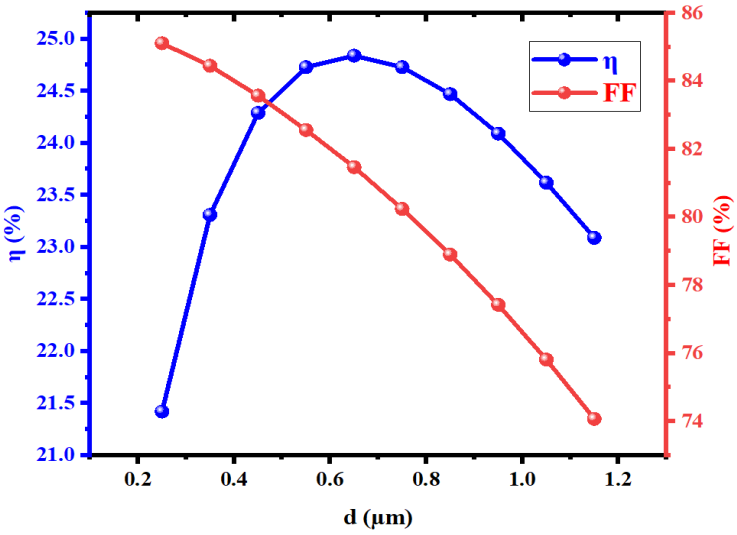

(b)

(a) ***[Data Table: https://rb.gy/xcif2]***
(b)*[Data Table: https://tinyurl.com/mm4fsddh]*

***Figure 21:* (a)** Effect of the Thickness of the p-CCZTSe absorption layer on the efficiency value (Η) and fill factor (FF); **(b)** Effect of the Thickness of the $CH_3NH_3Pb(I_{1-x}Cl_x)_3$ absorption layer on the efficiency value (Η) and fill factor (FF)

In ***figure 21:*(a)** Η increases from 22.75% to 25.04% when the thickness is 1µm after that it starts to decrease again continuously from 24.84% to 23.94% and FF increases from 81.58% to 81.88% when the thickness of the is 1 µm and then decreases again continuously from 81.51% to 79.74%.

In ***figure 21:*(b)** Η increases from 21.42% to 24.84%) when the thickness is 0.65µm after that it starts to decrease again continuously from 24.73% to 23.09% and FF increases from 85.11% to 81.47% when the thickness is 0.65 µm and then decreases again continuously from 80.24% to 74.07%.

❖ ***Effect of Acceptor Concentration***

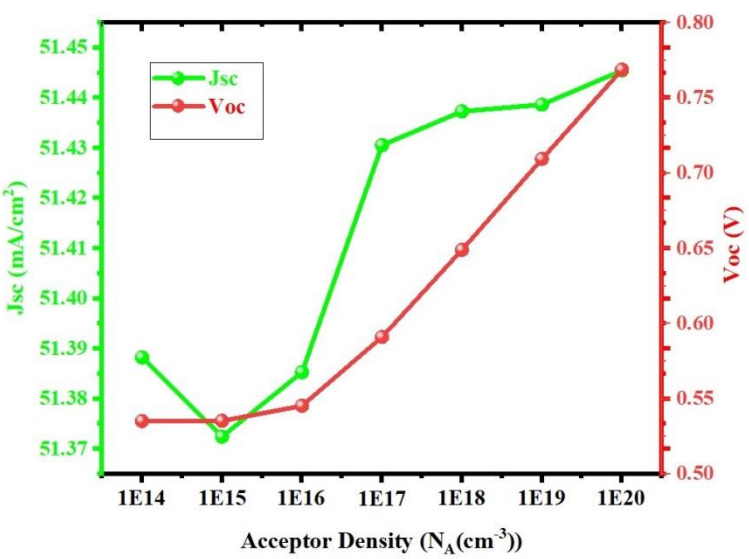

(a)

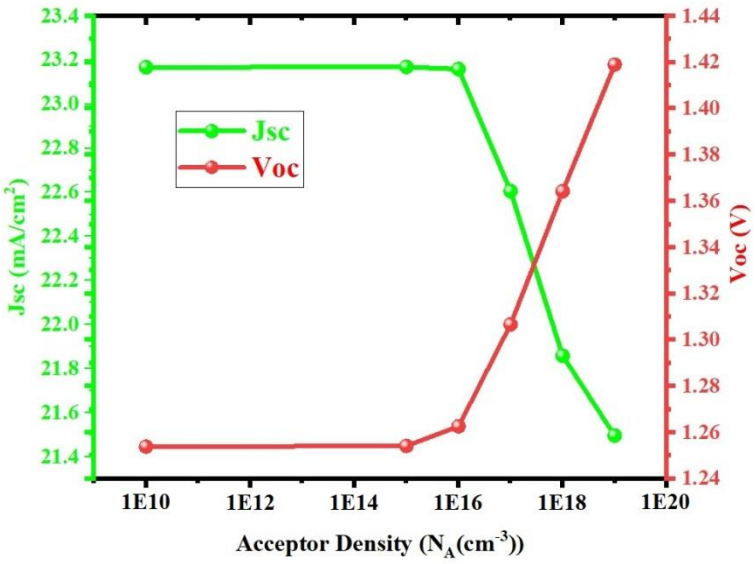

(b)

(a)*[Data Table: https://t.ly/KCdpL]*
(b)*[Data Table: https://tinyurl.com/5n7e2ct2]*

***Figure 22*: (a)** Effect of Acceptor Concentration in the absorption layer of p-CCZTSe layer on the current density (J_{SC}) and open circuit voltage (V_{OC}); **(b)** Effect of Acceptor Concentration in the $CH_3NH_3Pb(I_{1-x}Cl_x)_3$ layer on the current density (J_{SC}) and open circuit voltage (V_{OC})

In *figure 22*: (a) we can see that as acceptor density increases from 10^{14} cm^{-3} to 10^{20} cm^{-3}, V_{OC} increases continuously from 0.5351V to 0.7681V and J_{SC} also increases negligibly from 51.388231mA/cm^2 to 51.445444mA/cm^2.

In ***figure 22:* (b)** we can see that as acceptor density increases from 10^{10} cm^{-3} to 10^{19} cm^{-3}, V_{OC} increases continuously from 1.2539V to 1.419V and J_{SC} also decreases continuously from 23.168028 mA/cm^2 to 21.496134 mA/cm^2.

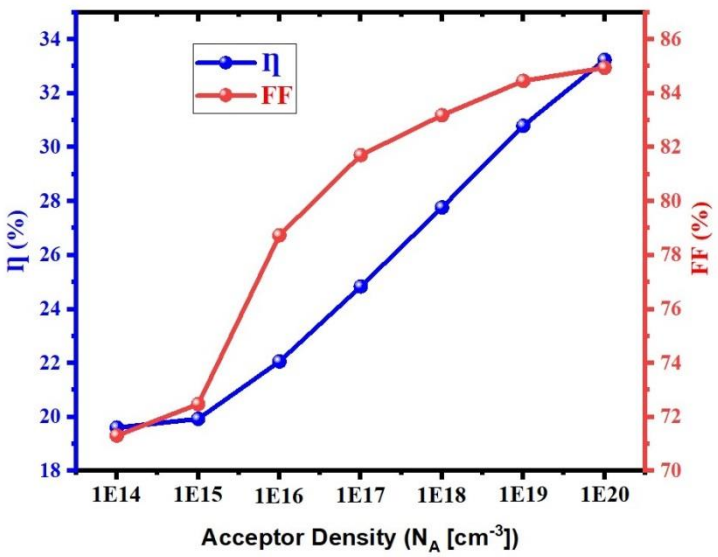

(a)

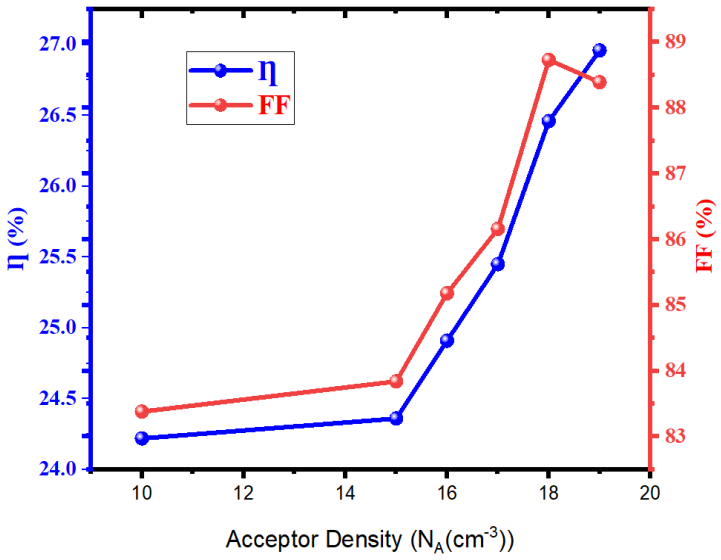

(b)

(a)*[Data Table: https://t.ly/KCdpL]*
(b)*[Data Table: https://tinyurl.com/5n7e2ct2]*

Figure 23: **(a)** Effect of Acceptor Concentration in the absorption layer on cell efficiency (ɳ) and filling factor (FF) of p-CCZTSe layer; **(b)** Effect of Acceptor Concentration in the absorption layer on cell efficiency (ɳ) and filling factor (FF) of $CH_3NH_3Pb(I_{1-x}Cl_x)_3$ layer

In ***figure 23:*****(a)** when the acceptor density is from 10^{14} cm^{-3} to 10^{20} cm^{-3}, ɳ increases from 19.61% to 33.24% and FF increases from 71.31% to 84.95% .

In ***figure 23:*****(a)** when the acceptor density is from 10^{10} cm^{-3} to 10^{19} cm^{-3}, ɳ increases from 24.22% to 26.96% and FF increases from 83.38% to 88.39%.

❖ ***Effect of Donor Concentration***

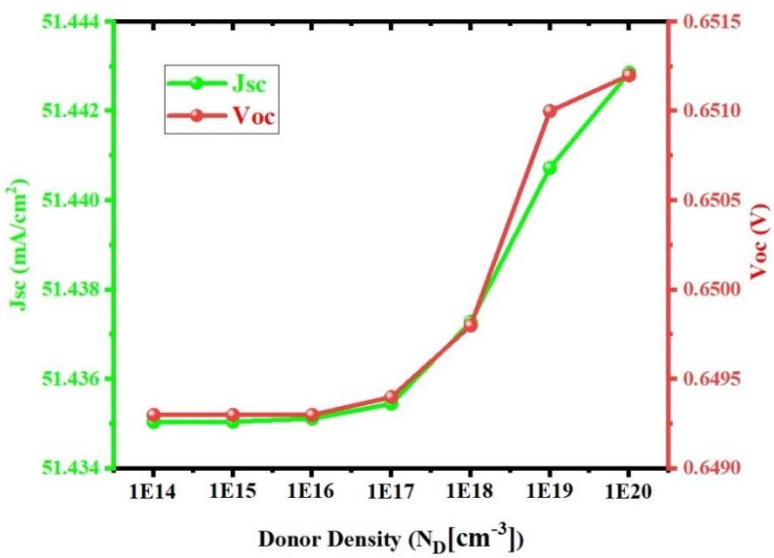

(a)

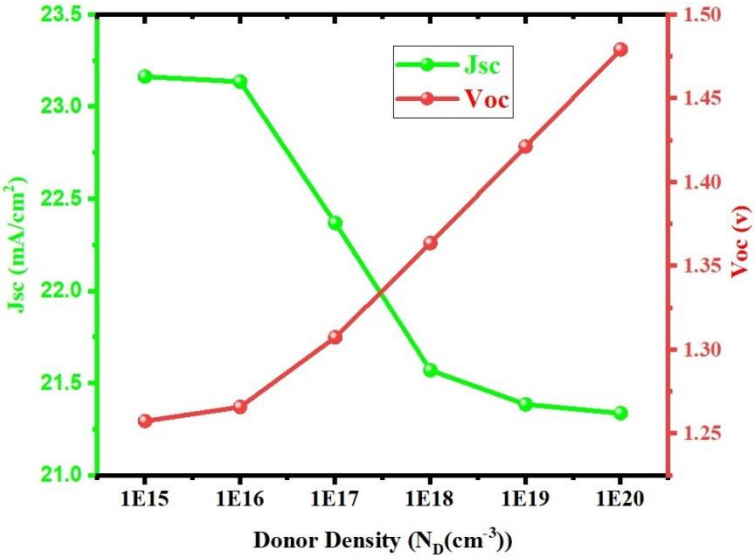

(b)

(a)*[Data Table: https://t.ly/6H7I_]*
(b)*[Data Table: https://tinyurl.com/58s7vha4]*

Figure 24: **(a)** Effect of donor concentration (N_D) in the n-CdS layer on V_{OC} and J_{SC}; **(b)** Effect of donor concentration (N_D) in the TiO_2 layer on V_{OC} and J_{SC};

In *figure 24*: **(a)** we can see that as donor density increases from 10^{14} cm^{-3} to 10^{17} cm^{-3}, V_{OC} increases negligibly from 0.6493V to 0.6498V and J_{SC} also increases negligibly from 51.388231mA/cm^2 to 51.445444mA/cm^2. After that, the donor density increases from 10^{18} cm^{-3} to 10^{20} cm^{-3}, V_{OC} and J_{SC} increases little bit.

In ***figure 24:*** **(b)** we can see that as donor density increases from 10^{15} cm^{-3} to 10^{20} cm^{-3}, V_{OC} increases continuously from 1.2576V to 1.4793V and J_{SC} also increases negligibly.

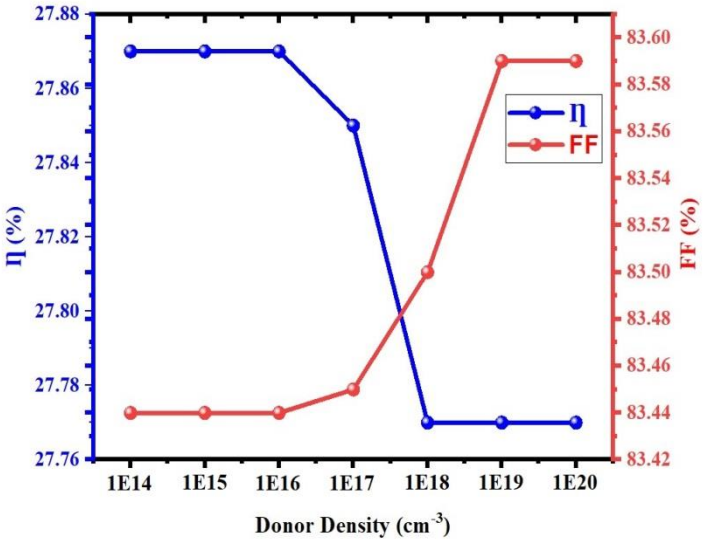

(a)

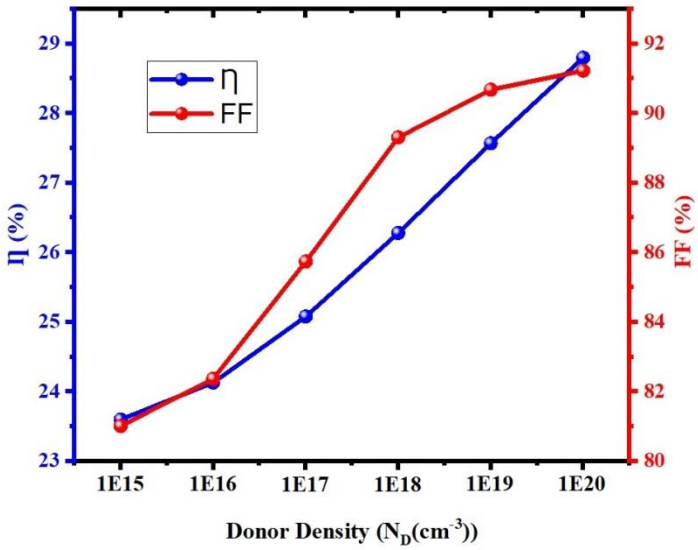

(b)

(a)*[Data Table: https://t.ly/6H7I_]*
(b)*[Data Table: https://tinyurl.com/58s7vha4]*

Figure 25: **(a)** Effect of the donor concentration (N_D) in the n-CdS layer on the cell efficiency (Ƞ) and the filling factor (FF); **(b)** Effect of the donor concentration (N_D) in the TiO_2 layer on the cell efficiency (Ƞ) and the filling factor (FF)

In ***figure 25:*****(a)** when the donor density is from 10^{18} cm^{-3} to 10^{20} cm^{-3}, Ƞ decreases little bit and FF negligibly increases when donor density is from 10^{14} cm^{-3} to 10^{20} cm^{-3}

In ***figure 25:*****(a)** when the donor density is from 10^{15} cm^{-3} to 10^{20} cm^{-3}, Ƞ increases continuously from 23.6% to 28.8% and FF increases from 81.01% to 91.23%.

❖ ***Effect of defects density in the absorbent layer***

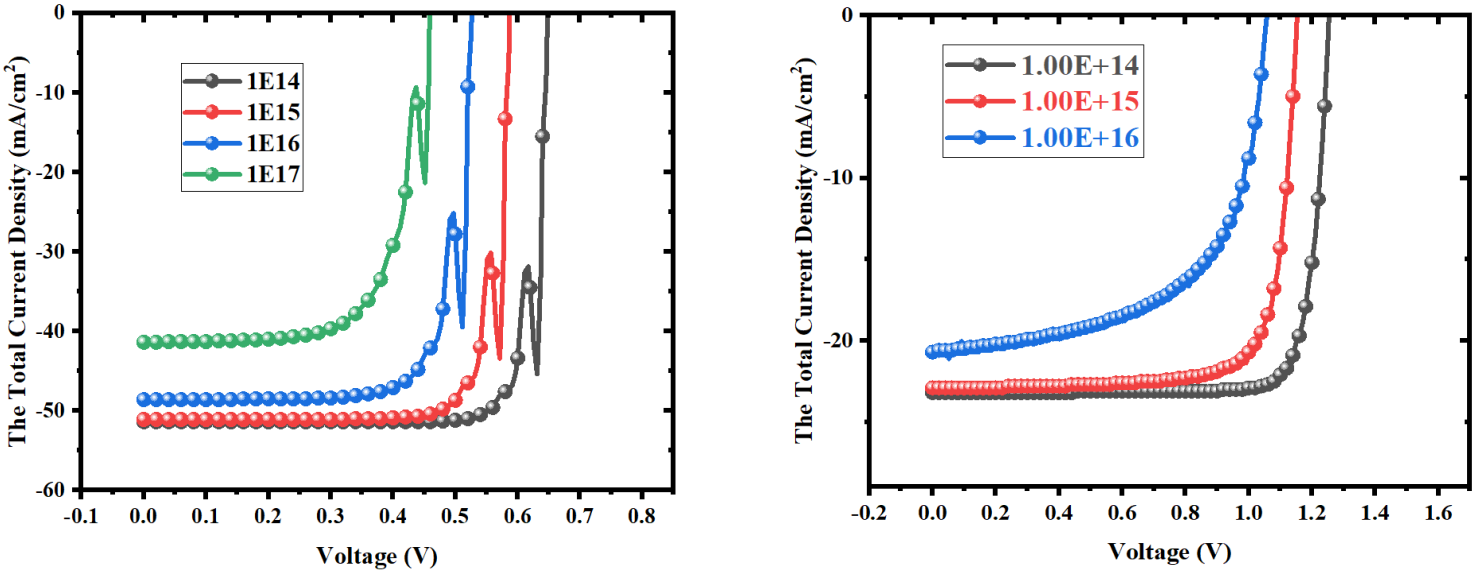

(a) (b)

(a)*[Data Table: https://t.ly/BYTIN]*
(b)*[Data Table: https://tinyurl.com/22jynpbb]*

Figure 26: **(a)** Effect of defect density in p-CCZTSe absorption layer on the I-V curve; **(b)** Effect of defect density in $CH_3NH_3Pb(I_{1-x}Cl_x)_3$ absorption layer on the I-V curve

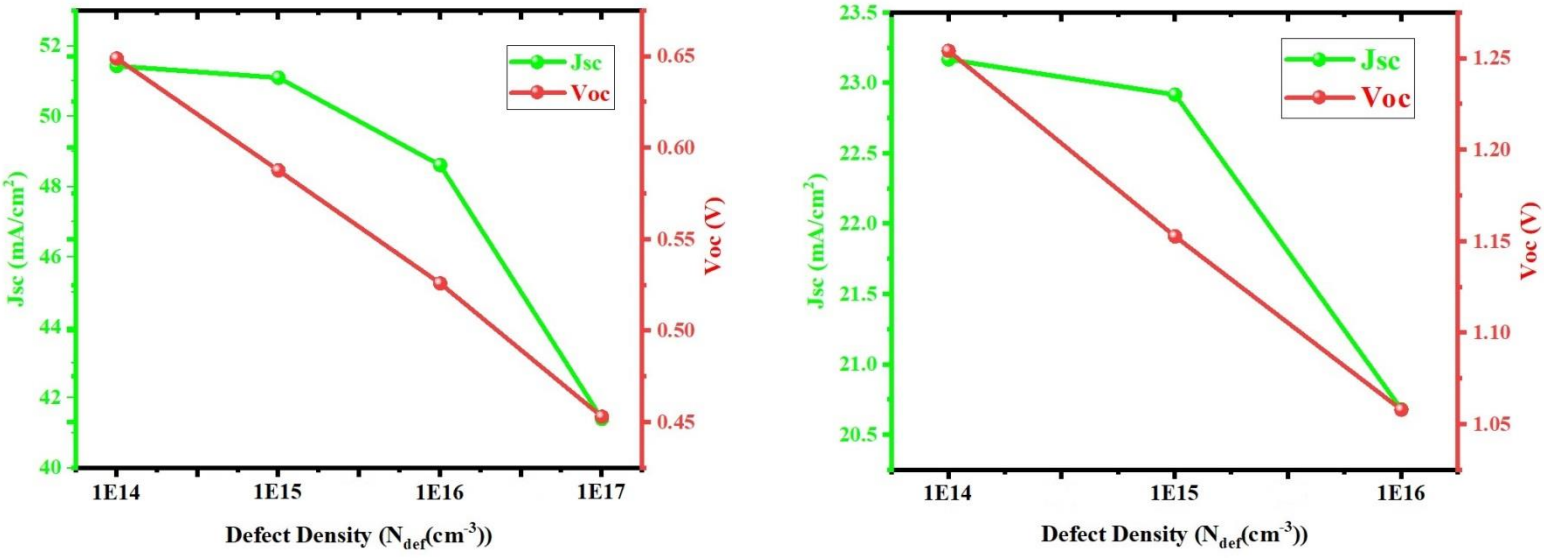

(a) (b)

(a)*[Data Table: https://t.ly/fqulu]*
(b)*[Data Table: https://tinyurl.com/9z8khk55]*

Figure 27: **(a)** Effect of the defect density in the p-CCZTSe absorption layer on V_{OC} and J_{SC}; **(b)** Effect of the defect density in the $CH_3NH_3Pb(I_{1-x}Cl_x)_3$ absorption layer on V_{OC} and J_{SC}

In *figure 27*: **(a)** we can see that as defect density increases from 10^{14} cm^{-3} to 10^{17} $cm^{-3}cm^{-3}$, V_{OC} decreases continuously from 0.649V to 0.4531V and J_{SC} also continuously decreases from 51.432857 mA/cm^2 to 41.400155 mA/cm^2.

In ***figure 27:*** **(b)** we can see that as defect density of the absorber layer increases from 10^{14} cm^{-3} to 10^{16} cm^{-3}, V_{OC} decreases continuously from 1.2542V to 1.058V and J_{SC} also decreases from 23.169198 mA/cm^{-3} to 20.681967 mA/cm^{-3}.

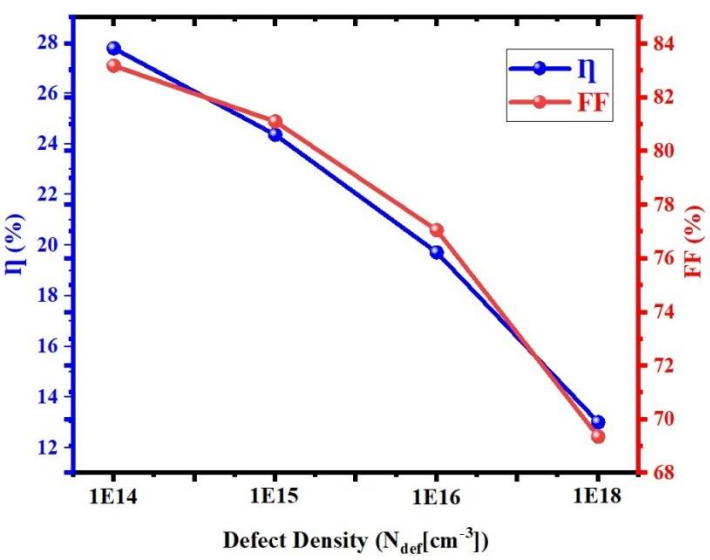

(a)

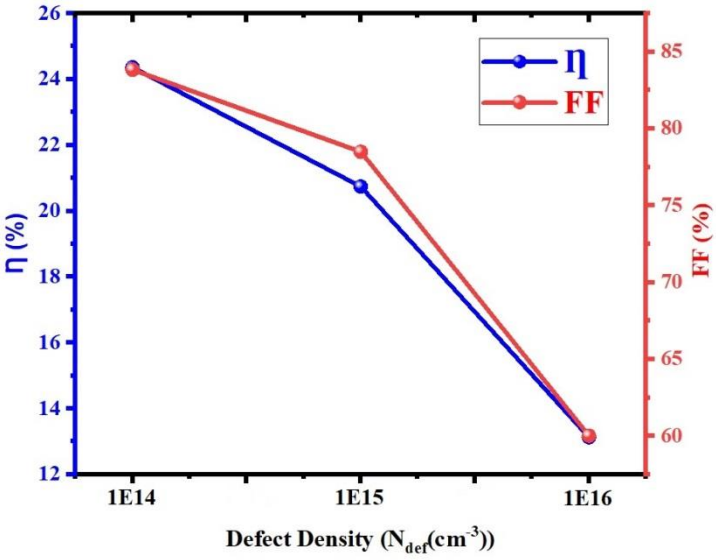

(b)

(a)*[Data Table: https://t.ly/fqulu]*
(b)*[Data Table: https://tinyurl.com/9z8khk55]*

Figure 28: **(a)** Effect of the defect density of the p-CCZTSe adsorption layer on the efficiency value (Ƞ) and fill factor (FF); **(b)** Effect of the defect density of the $CH_3NH_3Pb(I_{1-x}Cl_x)_3$ adsorption layer on the efficiency value (Ƞ) and fill factor (FF)

In ***figure 28:*** **(a)** when the defect density of the absorber layer is from 10^{14} cm^{-3} to 10^{17} cm^{-3}, Ƞ continuously increases from 27.77% to 13.01% and FF also increases from 83.19% to 69.36%.

In ***figure 28:*** **(b)** when the defect density of the absorber layer is from 10^{14} cm^{-3} to 10^{16} cm^{-3}, Ƞ decreases continuously increases from 24.36% to 13.13% and FF also decreases from 83.84% to 60.02%.

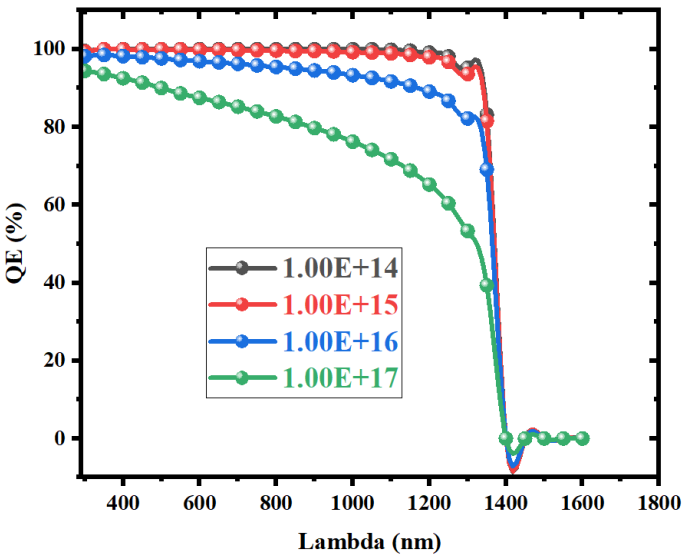

(a)

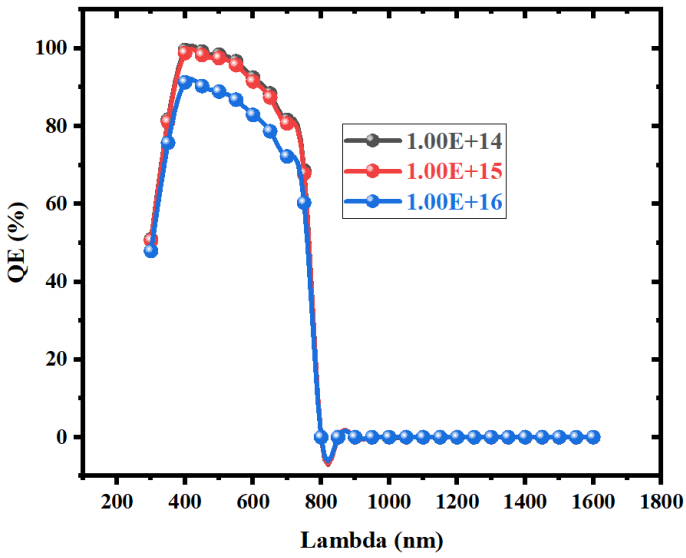

(b)

(a)*[Data Table: https://t.ly/5YJod]*
(b)*[Data Table: https://tinyurl.com/2w3a8uev]*

Figure 29: **(a)** Effect of defect density (N_{def}) on the Quantum efficiency (QE) of p-CCZTSe adsorption layer; **(b)** Effect of defect density (N_{def}) on the Quantum efficiency (QE) of $CH_3NH_3Pb(I_{1-x}Cl_x)_3$ adsorption layer.

❖ ***EFFECT OF TEMPERATURE***

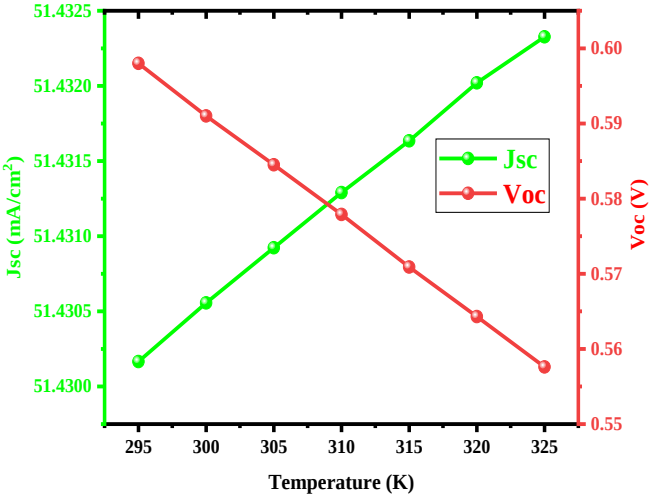

(a)

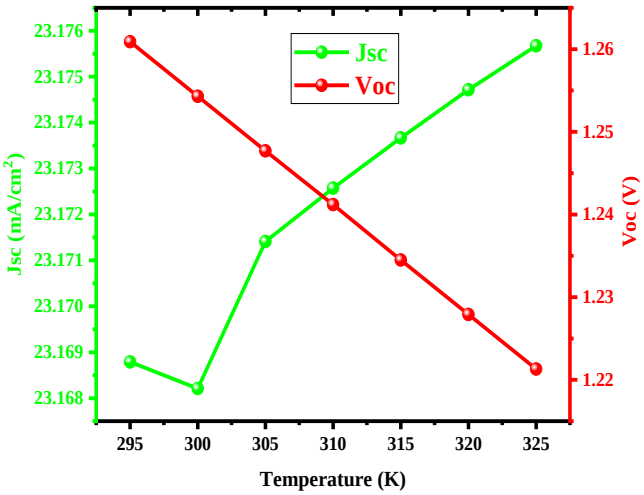

(b)

(a)*[Data Table: https://tinyurl.com/5cje42xy*
(b)*[Data Table: https://tinyurl.com/3jp4ccmy]*

Figure 30: **(a)** Effect of the Temperature in the p-CCZTSe based solar cell on V_{OC} and J_{SC}; **(b)** Effect of the Temperature in the $CH_3NH_3Pb(I_{1-x}Cl_x)_3$ based solar cell on V_{OC} and J_{SC}

In ***Figure 30:*** **(a)** we can see that as temperature increases from 295^{O}K to 325^{O}K, V_{OC} decreases little bit from 0.598V to 0.5576V and on the other hand J_{SC} increases little bit from 51.430166 mA/cm^2 to 41.432327 mA/cm^2.

In ***Figure 30:*** **(b)** we can see that as temperature increases from 295^{O}K to 325^{O}K, V_{OC} decreases little bit from 1.2609V to 1.2213V and on the other hand J_{SC} increases little bit from 23.168789 mA/cm^2 to 23.175673 mA/cm^2.

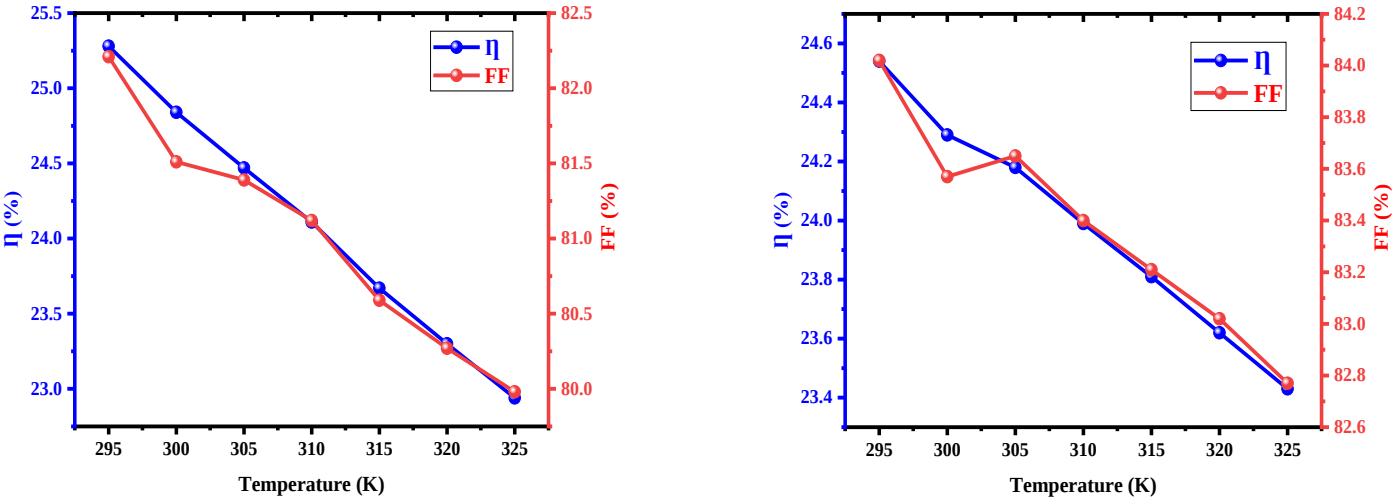

(a) (b)

(a)*[Data Table: https://tinyurl.com/5cje42xy]*

(b)*[Data Table: https://tinyurl.com/3jp4ccmy]*

Figure 31: **(a)** Effect of the Temperature in the p-CCZTSe based solar cell on the efficiency value (η) and fill factor (FF); **(b)** Effect of the Temperature in the $CH_3NH_3Pb(I_{1-x}Cl_x)_3$ based solar cell on the efficiency value (η) and fill factor (FF)

Figure 31: **(a)** we can see that as temperature increases from 295^{O}K to 325^{O}K, η continuously decreases from 25.28% to 22.94% and FF also decreases from 82.21% to 79.98%.

Figure 31: **(b)** we can see that as temperature increases from 295^{O}K to 325^{O}K, η continuously decreases from 24.54% to 23.43% and FF also decreases from 84.02% to 82.77%.

ANALYSIS

For CCZTSe based solar cell,

We can see that, when we increase the thickness the absorption layer notice that V_{OC} continuously decreased and J_{SC} increased. On the other hand, FF and η increases and decreases with increasing thickness. If we theoretically want to find out these values, then we will use equation (*i* – *v*).

Again when changing the acceptor density of the absorption layer the values of V_{OC}, J_{SC}, η & FF increase continuously.

When changing the donor density of the buffer layer (CdS), the values of V_{OC}, J_{SC}, η & FF increase little bit.

When changing the defect density of the absorption layer, the values of V_{OC}, J_{SC}, ɳ & FF decrease continuously.

When changing the temperature in the p-CCZTSe based solar cell, the values of V_{OC}, ɳ & FF decreases and the value of J_{SC} increases little bit.

For $CH_3NH_3Pb(I_{1-x}Cl_x)_3$ based solar cell,

We can see that, when we increase the thickness the absorption layer notice that V_{OC} continuously decreased and J_{SC} increased. On the other hand, FF and ɳ increases and decreases with increasing thickness. If we theoretically want to find out these values, then we will use equation (*i – v*).

Again when changing the acceptor density of the absorption layer the values of V_{OC}, J_{SC}, ɳ & FF increase continuously.

When changing the donor density of the buffer layer (TiO_2), the values of V_{OC}, J_{SC}, ɳ & FF increase little bit.

When changing the defect density of the absorption layer, the values of V_{OC}, J_{SC}, ɳ & FF decrease continuously.

When changing the temperature in the $CH_3NH_3Pb(I_{1-x}Cl_x)_3$ based solar cell, the values of V_{OC}, ɳ & FF decreases and the value of J_{SC} increases little bit.

In the case of solar cells, the higher the efficiency of the solar cell, the better the solar cell. Considering the above results, we believe that CCZTSe based solar cells are better because of CCZTSe based solar cell efficiency is higher than $CH_3NH_3Pb(I_{1-x}Cl_x)_3$ efficiency when acceptor density is 10^{20} and thickness constant is 1.25 µm.

On the other hand if we think about environment then 2nd solar cell will be better because 2nd solar cell does not contain CdS which is present in 1st solar cell. Cadmium sulfide (CdS) is a material commonly used in thin-film solar cells, particularly in the context of certain photovoltaic technologies like cadmium telluride (CdTe) solar cells. While CdS-based solar cells can offer certain advantages such as low cost and high efficiency, there are also environmental concerns associated with the use of cadmium, a heavy metal, in these devices. Cadmium is classified as a hazardous substance due to its toxic nature and potential to bio accumulate in ecosystems. During the manufacturing, use, and disposal of CdS-based solar cells, there is a risk of cadmium being released into the environment. Cadmium is known to be harmful to human health, especially if ingested or inhaled. Prolonged exposure to cadmium can lead to various health issues, including lung and prostate cancers, kidney damage, and bone diseases. Workers in solar cell manufacturing and recycling facilities may be particularly at risk if proper safety measures are not in place.

If we consider temperature then in low temperature like $295^{O}K$ p-CCZTSe based solar cell has good efficiency(25.28%) and on the other hand in high temperature ($325^{O}K$) $CH_3NH_3Pb(I_{1-x}Cl_x)_3$ based solar cell has good efficiency (23.43%).

If we consider efficiency then 1st solar cell (p-CCZTSe based solar cell) is best and if we consider environment then 2^{nd} ($CH_3NH_3Pb(I_{1-x}Cl_x)_3$ based solar cell) solar cell will be better. 2^{nd} ($CH_3NH_3Pb(I_{1-x}Cl_x)_3$ based solar cell) solar cell has a good efficiency of 26.96% when thickness is 0.45 µm, acceptor density is 10^{19} and defect density is 10^{14}.

CONCLUSION

The simulation study using the SCAPS-1D program for CCZTSe thin-film solar cells yielded significant insights. The model accurately captured the device behavior and performance. Efficiency was found to be promising under certain conditions. However, challenges like material quality and interface engineering need attention for practical application. Overall, the study highlights CCZTSe's potential for solar cells while emphasizing the importance of optimizing material properties to enhance performance.

FUTURE WORK PLANS

If we had more time to continue the project, we could have simulated the acceptor density, donor density, temperature, defect density for different layers. We'll try to figure out these values next time.

REFERENCE

1. Kareem, W. Y. A. and M. Q. (2022). Simulation of Thin-Film Solar Cells based on (CCZTSe) Using (SCAPS-1D) Program. *JOURNAL of ALGEBRAIC STATISTICS*, *13*(2), 902–913. https://doi.org/10.52783/jas.v13i2.241
2. Rai, S., Pandey, B.K. and Dwivedi, D.K. (2020). Modeling of highly efficient and low cost CH3NH3Pb(I1-xClx)3 based perovskite solar cell by numerical simulation. *Optical Materials*, 100, p.109631. doi: https://doi.org/10.1016/j.optmat.2019.109631.
3. Patel, A. K., Rao, P. K., Mishra, R., & Soni, S. K. (2021). Numerical study of a high-performance thin film CIGS solar cell with a-Si and MoTe2 hole transport layer. *Optik*, *243*, 167498. https://doi.org/10.1016/j.ijleo.2021.167498
4. Boudour, S., Bouchama, I., Laidoudi, S., Bedjaoui, W., Lamiri, L., Belgherbi, O., & Aziez, S. (2022). Study of CIGS Pseudo-Homojunction Thin Film Solar Cell using SCAPS-1D. *East European Journal of Physics*, *4*, 145–152. https://doi.org/10.26565/2312-4334-2022-4-14
5. Sadanand, & Dwivedi, D. K. (2020). Numerical Simulation for Enhancement of the Output Performance of CZTS Based Thin Film Photovoltaic Cell. *Advanced Science, Engineering and Medicine*, *12*(1), 88–94. https://doi.org/10.1166/asem.2020.2526
6. Zyoud, S. H., Zyoud, A. H., Ahmed, N. M., Prasad, A. R., Khan, S. N., Abdelkader, A. F. I., & Shahwan, M. (2021). Numerical Modeling of High Conversion Efficiency FTO/ZnO/CdS/CZTS/MO Thin Film-Based Solar Cells: Using SCAPS-1D Software. *Crystals*, *11*(12), 1468. https://doi.org/10.3390/cryst11121468
7. Simulation of Lead based Perovskite on SCAPs 1D simulator. (n.d.). Www.youtube.com. Retrieved August 16, 2023, fromhttps://www.youtube.com/watch?v=atbw2PDpH-c&list=PLenEAMrv82IBnkIDIDtQgw1VUO6lllb38

8. Ijrer.org. (2023). Available at: https://www.ijrer.org/ijrer/index.php/ijrer/article/view/6182 [Accessed 20 Aug. 2023].